



The Ministry of National Infrastructures
Geological Survey of Israel

Amos Salamon

Report GSI / 30 / 04
Jerusalem, December 2004

**Seismically induced ground effects of the February 11, 2004,
 $M_L = 5.2$, northeastern Dead Sea earthquake**



THE MINISTRY OF NATIONAL INFRASTRUCTURES
GEOLOGICAL SURVEY OF ISRAEL

Seismically induced ground effects of the February 11, 2004, $M_L=5.2$, northeastern Dead Sea earthquake

Amos Salamon

With contributions by:

Meir Abelson¹, Rivka Amit¹, Shlomo Ashkenazi¹, Yoav Avni¹, Gideon Baer¹, Ze'ev B. Begin¹,
Carmi Zion¹, Onn Crouvi¹, Yehuda Enzel², Lea Feldman³, Itai Gavrieli¹, Zohar Gvirtzman¹,
Yariv Hamiel¹, Haim Hemo¹, Rami Hofstetter³, Oded Katz¹, Tomy Magdalen¹, Uri Malik¹,
Yoav Nachmias¹, Naomi Porat¹, Josh Steinberg¹, Gideon Steinitz¹, Tuncay Taymaz⁴,
Rami Weinberger¹, Yoseph Yechieli¹, Seda Yolsal⁴ and Ezra Zilberman¹

¹ Geological Survey of Israel, 30 Malkhe Yisrael Street, Jerusalem 95501, Israel

² Institute of Earth Sciences, Hebrew University of Jerusalem 91904, Israel

³ The Geophysical Institute of Israel, P.O. Box 182, Lod, 71100, Israel

⁴ Seismology Section, Istanbul Technical University, Maslak, 80626, Istanbul, Turkey

Table of Contents

ABSTRACT	1
1 INTRODUCTION	2
1.1 EARTHQUAKE INDUCED GROUND EFFECTS	3
1.2 PREVIOUS REPORTS ON SEISMICALLY INDUCED GROUND EFFECTS	3
1.3 GEOLOGY OF THE AFFECTED AREA	4
2 THE 11/02/04 EARTHQUAKE	5
2.1 SEISMOTECTONICS.....	5
2.1.1 The main event	5
2.1.2 The main shock mechanism	5
2.1.3 The aftershock sequence.....	8
2.2 EARTHQUAKE INDUCED GROUND EFFECTS	9
2.2.1 Cracks	9
2.2.2 Slope failure.....	10
2.2.3 Liquefaction.....	11
2.2.4 Tsunami	12
2.2.5 Sinkholes	12
2.2.6 Water level in wells	13
2.2.7 Radon flux	14
2.2.8 Other natural effects	14
2.2.9 Doubtful effects	14
3 DISCUSSION	15
3.1 FAILURE EFFECTS AND VULNERABILITY OF THE YOUNG FORMATIONS ...	16
3.2 EARTHQUAKE INTENSITIES - THE INQUA EEE SCALE.....	17
3.3 POST EARTHQUAKE INVESTIGATIONS.....	18
4 CONCLUSIONS	19
5 ACKNOWLEDGMENTS	20
6 REFERENCES	21

List of Figures

- Figure 1 Map of the 11/2/2004 earthquake sequence and the associated events
- Figure 2 All $M_L \geq 3$ recorded events of the last 80 years in and around the Dead Sea
- Figure 3 Typical section of the Ze'elim Formation
- Figure 4 First motion fault plane solution of the main shock, by GII
- Figure 5 Waveform inversion fault plane solution of the main shock, by ITU
- Figure 6 CMT of the main shock, by EMSC
- Figure 7 Location map of the seismically induced ground effects
- Figure 8 A detailed map of the seismogenic cracks along the Darga coast
- Figure 9 Granulometric analysis of a sample of a liquefied material
- Figure 10 Change of water level in the Radon 1 and 2 and the Mineral 1 and 2 wells
- Figure 11 Radon flux registered by two of the Enot Zuqim monitors
- Figure 12 Moment magnitude versus distance for slope failure
- Figure 13 Moment magnitude versus distance for liquefaction
- Figure 14 INQUA EEE intensity map

List of Tables

- Table 1 Parameters of the main shock
- Table 2 Parameters of the main shock mechanism
- Table 3 List of main events and aftershocks
- Table 4 List of the seismically induced ground effects
- Table 5 Change of water level in wells

List of Photos

- Photo 1 Open cracks in the alluvial deposits of N. Og, near the Qalya coast
- Photo 2 Arcuate cracks along a slump margins, Qalya coast
- Photo 3 Open cracks with vertical offset, N. Darga
- Photo 4a Reopened cracks oriented oblique to the shoreline, Qalya coast
- Photo 4b Reopened cracks oriented parallel to the shoreline, Darga coast
- Photo 5a Seismogenic crack superimposed on mud cracks, Darga coast
- Photo 5b Pattern of the seismogenic crack is not identical with the mud crack
- Photo 6a A slump at the modern sea cliff near the waterfront of the Qalya coast
- Photo 6b A slump of a bank in the gully that drains the Hamme En Gedi hot springs

- Photo 7 Collapse of a gully bank of N. Ze'elim
- Photo 8 Collapse of a modern sea cliff that faces the waterfront of the Qalya coast
- Photo 9 Collapse of hard carbonate rocks of the Judea Group, N. Arugot
- Photo 10 The artificial trench in the Qalya coast, where liquefaction occurred
- Photo 11 Mud cones and open cracks inside the artificial trench, Qalya coast
- Photo 12 Injected mud along an open crack, Darga coast
- Photo 13 Wet sediment around a boulder, Darga coast
- Photo 14 Waves and an unusual line in the Dead Sea half an hour after the event
- Photo 15 Ponds along the Darga coast, probably formed by the tsunami wave
- Photo 16 Tsunamite and a reopened crack, Darga coast.
- Photo 17a Ponds in one of the Shalem 2 sinkholes, south of Mineral Beach
- Photo 17b Stream lines and open cracks at the bottom of a sinkhole, Shalem 2 site
- Photo 18 Turbidities along the coast between En-Gedi and Darga coast

Appendices

- Appendix 1 The proposed “INQUA EEE scale” (Michetti et al., 2004)
- Appendix 2 Categories used for the analysis of secondary ground effects
- Appendix 1 INQUA EEE scale field survey form

ABSTRACT

The moderate earthquake of February 11, 2004, $M_L=5.2$, occurred in the northeastern segment of the Dead Sea at a depth of 17 km. Fault plane solution shows a transtensional mechanism with a sinistral plane that strikes NNW and a dextral plane that trends E-W. Although in general this mechanism accords with the nature of the Dead Sea Rift, none of the nodal planes coincide with a known structure in that area. The aftershocks were clustered west of the main shock, along WNW direction, suggesting the right lateral plane as the preferred rupture plane. If so, it may reflect the seismogenic activity of an intra-basinal structure.

The earthquake induced a wealth of ground effects. Exploration of the northwestern Dead Sea coast immediately after the event revealed various phenomena as far as 40 km away from the epicenter, mostly in the soft Holocene deposits:

- a. Cracks that may relate to gravitational sliding, differential compaction and reopening of tectonic joints.
- b. Landslides along the modern sea cliffs; collapse of gully and channel banks; sporadic rock falls.
- c. Liquefaction in an artificial trench; injected mud in an open crack, and wet sediment around boulders.
- d. A tsunami up to a meter high and a rough sea in the northern Dead Sea basin.
- e. A water level rise of 20-30 cm in some wells as well as a small drop in others; a sudden drop of about a meter in the water level in a few sinkholes. However, a lack of continuous recording does not enable us to determine the exact timing of the change.
- f. A change of radon concentration in two of the Enot Zuqim monitors, 14 hours before the earthquake.
- g. Dust, loud noise, wavy motion of the ground and shaking palm trees.

Of all units, the Ze'elim Formation was the most severely affected. It therefore seems to be the weakest geotechnical unit in the region and thus the most vulnerable one. According to the newly proposed "INQUA EEE scale" that grades the intensity of natural effects, the maximum degree reached is VI. These effects tend to fade away and become indistinguishable, and hence should be detected immediately after the earthquake.

1 INTRODUCTION

A moderate earthquake was felt in Israel, Jordan and nearby countries on February 11, 2004, 08:15AM UTC (10:15AM local time). The focus was in the northeastern Dead Sea, at 31.7N 35.55E, at a depth of 17 km. Local magnitude (M_L) of the main shock was 5.2 (Feldman et al., 2004) and was followed by aftershock activity (Geophysical Institute of Israel (GII) data; Wust-Bloch and Lazar, 2004) (Fig. 1).

Seismic activity along the Dead Sea Transform (DST) is well known from paleoseismological evidence (Reches and Hoexter, 1981; Marco et al., 1997; Neimi, 1997; Amit et al., 1999; Zilberman et al., 2000; Klinger et al., 2000a, 2000b), seismites and ground effects (Wachs and Levitte, 1981, 1984; El Isa and Mustafa, 1986; Niemi and Ben-Avraham, 1994; Marco and Agnon, 1995), historical documents (Amiran et al., 1994 and references therein) and instrumental recordings (mainly International Seismological Summary (ISS) (1918-1963); International Seismological Centre (ISC) (1964-1993, 1991, 2000); Institute for Petroleum Research and Geophysics (IPRG) (1982-1993); and GII (1996, internet website, Bulletins). This activity seemed to have reached a maximal magnitude of about 7-7.5. The seismicity along the DST is concentrated mostly along the deep basins of the Gulf of Elat, the Dead Sea and the Sea of Galilee (van Eck and Hofstetter, 1990; Salamon et al., 1996; Shapira, 1997). In fact, the 11/2/2004 earthquake was the sixth $M_L \geq 5$ event recorded in and around the Dead Sea basin during the last century (Fig. 2). This basin is the largest inland pull-apart structure along the DST (Garfunkel, 1981; Garfunkel and Ben-Avraham, 2001). Thus, neither the occurrence of this event, nor its location and magnitude, was exceptional. However, exploration of the Dead Sea coasts immediately after the earthquake revealed a wealth of earthquake-induced ground effects that were hardly documented in Israel after former moderate events.

The time span between strong earthquakes in this region is large (Rotstein, 1987) and therefore it is necessary to obtain maximum data from the moderate shocks that hit the region from time to time. Though extrapolating ground response in moderate events onto a strong shaking is not necessarily linear, this occasion is still an invaluable opportunity to document the resulting effects and characterize the nature of the ground around the epicentral area.

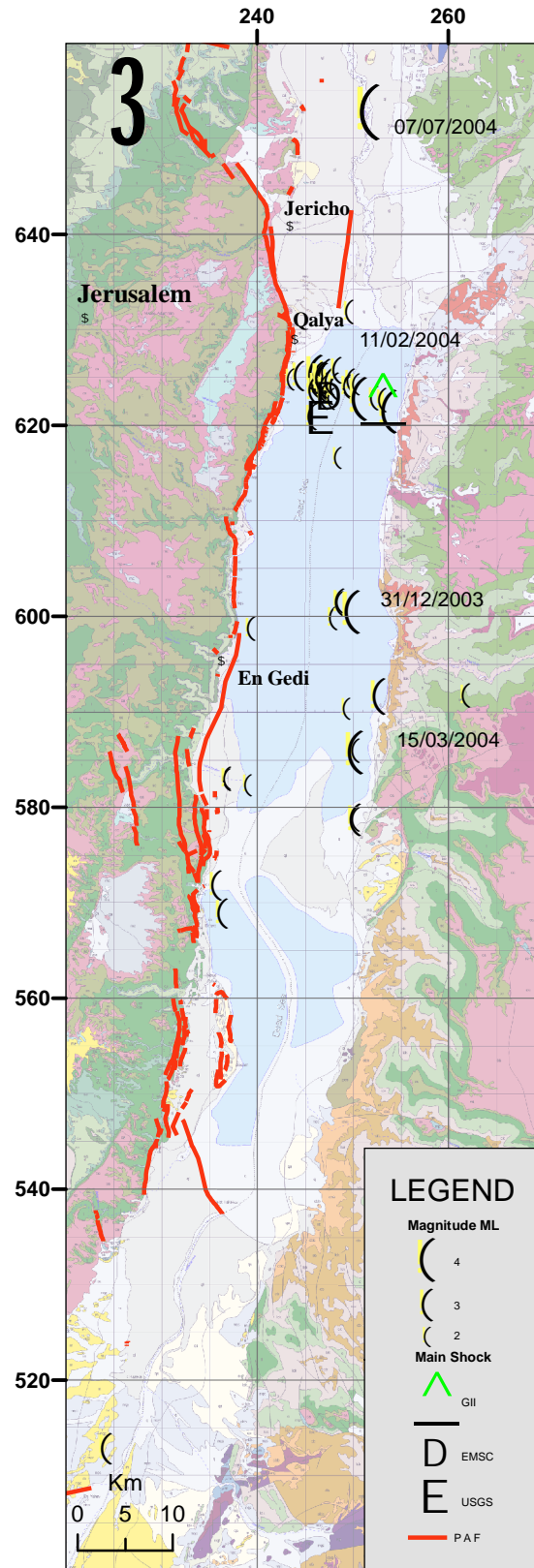


Fig. 1. Map of the 11/2/2004 earthquake sequence and the associated events during the time period 1/1/2003-30/9/2004 (GII catalog), superimposed on the geological map (Sneh et al., 1998). Note that most of the activity is concentrated along the northeastern margins of the Dead Sea. EMSC and USGS main shock epicenter locations are also shown. Potentially Active Faults (PAF) relate only to the western side of the Dead Sea while the eastern side has not been yet mapped.

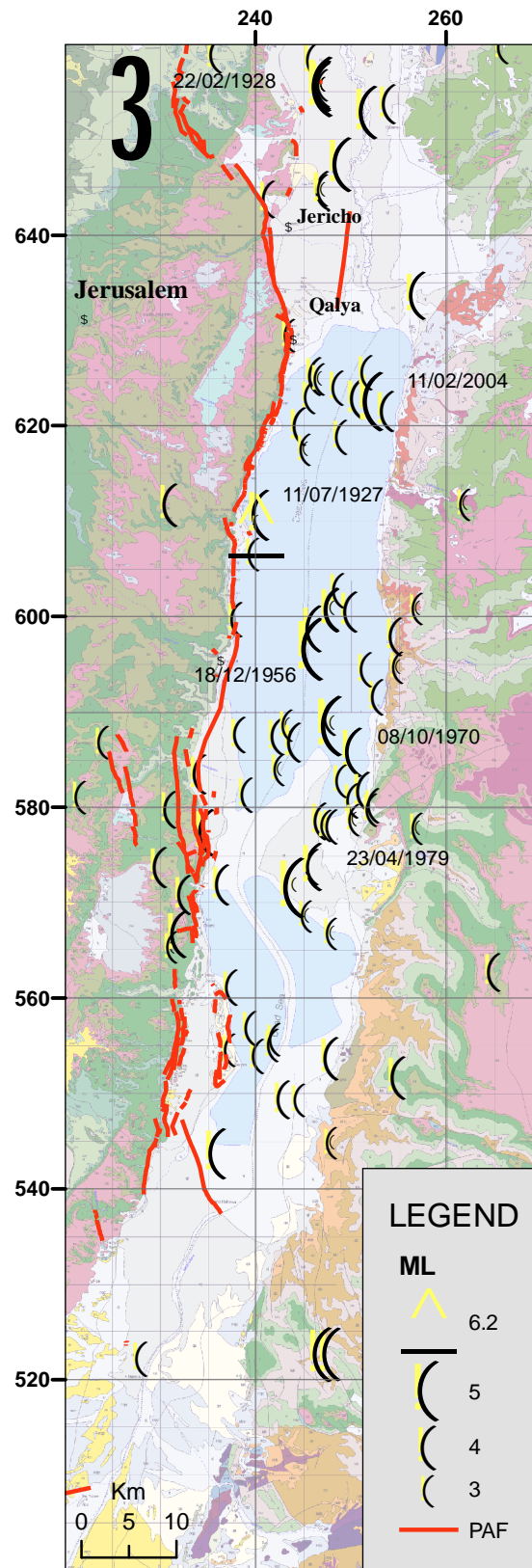


Fig. 2. All $M_L \geq 3$ recorded events of the last 80 years in and around the Dead Sea, superimposed on the geological map (Sneh et al., 1998). Data is taken from the GII catalog that seems to be complete for this threshold during the last 25 years. Potentially active faults (PAF) relate only to the western side of the Dead Sea, the eastern side has not been yet mapped.

1.1 Earthquake induced ground effects

Earthquakes cause many environmental effects. These can be classified under various subjective categories such as natural phenomena (e.g., ground failure, hydrological anomalies), hazardous factors (e.g., surface faulting, site amplification), macroseismic effects (e.g., damage to man-made structures) and others. Here we concentrate on the natural effects, with an emphasis on the hazard factors that may put at risk man-made structures. Study of these factors in Israel has been based mainly on worldwide experience. The 11/2/04 event however, is an opportunity to observe natural effects that are typical of the Dead Sea area and thus improve our evaluation of seismic hazards in that area in particular.

1.2 Previous reports on seismically induced ground effects in Israel

Earthquake induced ground effects in Israel were already reported in regard to strong events. Prehistoric seismites in the Lisan deposits near the Dead Sea were described by El-Isa and Mustafa (1986) and Marco and Agnon (1995). Amiran et al. (1994, and references therein) mentioned tsunamis along the Mediterranean coast, seiches in the Dead Sea and the Sea of Galilee, blockage of the flow of the Jordan River because of a landslide of the Lisan marl and floating of large asphalt blocks in the Dead Sea. The last strong earthquake in the Dead Sea, July 11, 1927, $M=6.2$, caused cracks in the ground of the Jordan valley and near the Dead Sea, a stop of the flow of the Jordan River by a landslide, and a seiche in the Dead Sea (Amiran et al., 1994; Ben-Menahem et al., 1976; Avni, 1999). More comprehensive documentation of failure features of cracks and joints, rockfalls, sandblows, tsunami, breaking of coral reefs, as well as water level fluctuations, dust and noise, was collected by Wust (1997) after the $M_w=7.2$, November 22, 1995, Nuwieba earthquake. It is interesting to note that some biblical descriptions may have already associated some natural phenomena with strong earthquakes (e.g., Shalem 1949; Bendor, 1989 and Nur, 1991), though not necessarily as a cause and effect.

While these descriptions are all related to strong earthquakes, ground effects caused by moderate events are barely described. Shalem (1945) discussed whether the whitening

of the Dead Sea in the summer of 1943 was related to the September 10, 1943, $M_L=4.7$ earthquake located east of the Dead Sea. Arieh et al. (1977) mentioned landslides and a rock avalanche after the Jordan Valley earthquake of September 3, 1973, $4\frac{1}{2}$ Richter magnitude, and Arieh et al. (1980, 1982) reported slumping of shale beds and talus as a result of the Dead Sea earthquake of April 23, 1979, $m_b=5.1$.

1.3 Geology of the affected area - the northwestern Dead Sea coast

Nearly all of the seismic effects of the February 11, 2004 event were found within the Dead Sea pull-apart basin, along the northwestern coast of the lake. Most affected of all was the uppermost unit that was deposited during the Holocene in the lake that occupied the basin and by floods that deposited alluvial material interbedded with the lake sediments. This unit is the Ze'elim Formation (Yechieli et al., 1993; Ken-Tor et al., 2001) and it consists of unconsolidated laminated deposits of soft detritus and evaporites (mainly aragonite) that are intercalated landward with unconsolidated alluvial material (Fig. 3). The unit is being exposed in recent years because of the continuous drop of the Dead Sea water level and retreat of the waterfront. The water table near the lake is shallow and water discharges in many places close to the shoreline; therefore, the water content in this unit is high.

Overall, the soft (weak) lithology, high water content and young age of the Ze'elim Formation are of critical importance in determining its geotechnical nature and consequently its response to seismic accelerations.

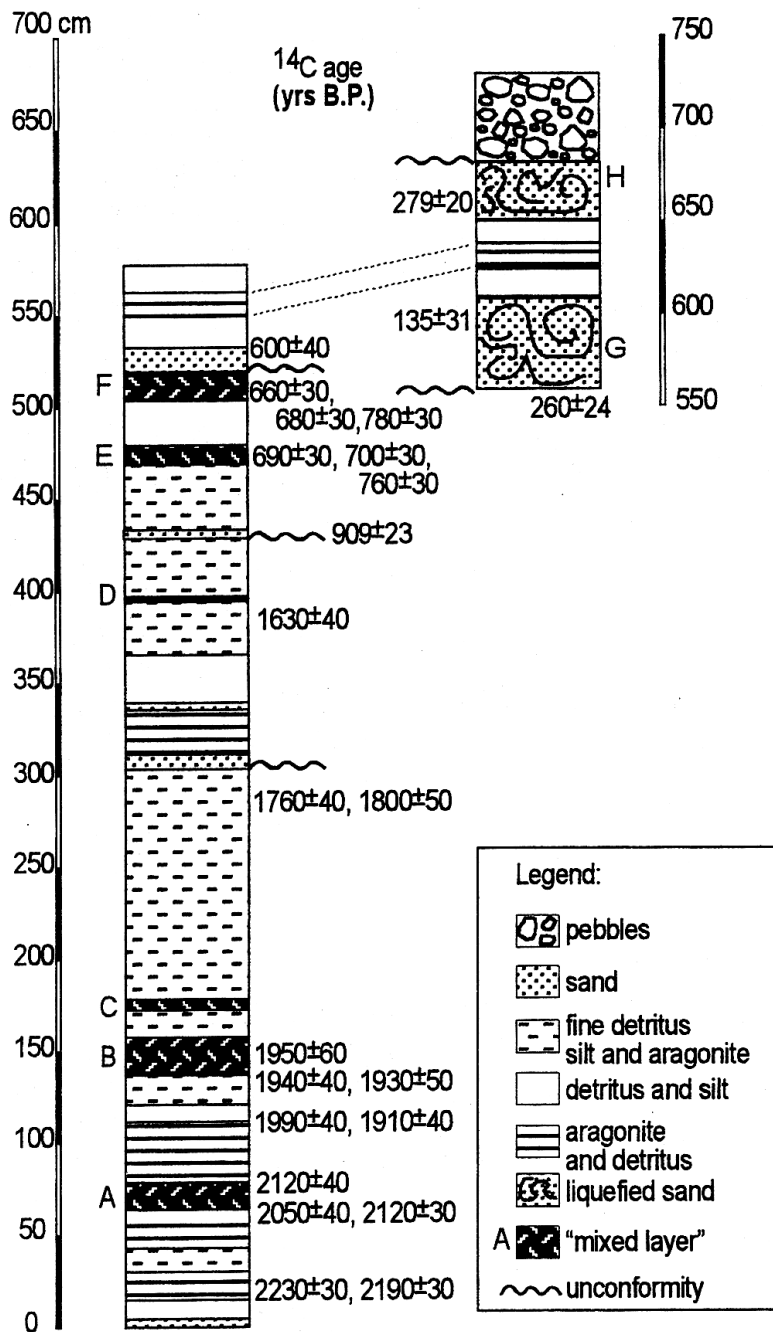


Fig. 3. The lithology and chronology of a composite section exposed in the Ze'elim plain. The section is described from two outcrops exposed in different gullies 300m apart (Ken-Tor et al., 2001).

2 THE 11/02/04 EARTHQUAKE

2.1 Seismotectonics

2.1.1 The main event

The earthquake occurred on February 11, 2004, 08:15AM UTC, in the northeastern Dead Sea and was followed by a sequence of aftershocks. The earthquake parameters as determined by the GII, European-Mediterranean Seismological Centre (EMSC) and the United States Geological Survey (USGS) institutes are presented in Table 1.

Table 1. Parameters of the main shock

* Source of data / parameter	GII	EMSC	USGS
Origin time (UTC)	08:15:03	08:15	08:15:03
Magnitude	5.2 (M _L) 5.1 (mb) 5.2 (M _m)	5.1 (mb)	5.1 (M)
N	31.7	31.70	31.68
E	35.56	35.50	35.49
Depth (km)	17	15	25.8

* Source of data:

GII: <http://www.gii.co.il/heb/default.html>

EMSC: http://www.emsc-csem.org/cgi-bin/ALERT_alertfile.sh?S0841&INFO

USGS: http://neic.usgs.gov/neis/eq_depot/2004/eq_040211/neic_etal_m.html

2.1.2 The main shock mechanism

Three different fault plane solutions of the main shock were available, all of them pointing towards a similar transtensional mechanism (Figs 4, 5, 6 and Table 2):

A. First motion solution based on first P-wave arrivals is presented in Figure 4 and

```

main
040211 815 3.24 31-41.88 35-33.18 16.00 5.20 41 303 10 203
80 170 70-140 -27 63 52 -25 0.09 53 8.15 0.75 0.00 5 15 10 b|a

```

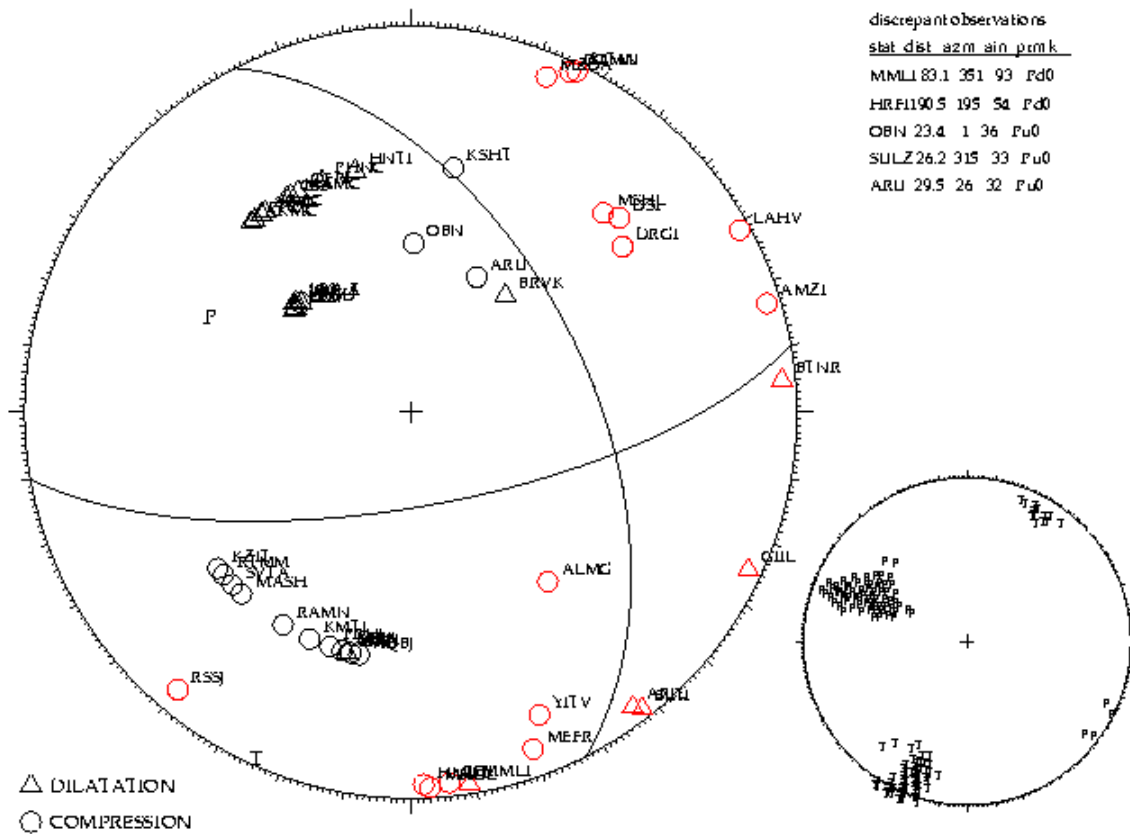


Fig. 4. First motion fault plane solution of the main shock (by R. Hofstetter, GII). The values above the focal sphere show the origin time, geographical coordinates, depth, magnitude, trend and dip of P & T axes, strike, dip direction, dip and rake of the nodal planes, and quality parameters. The parameters are also listed in Table 2. Stations that does not match the solution are listed on the upper right side and uncertainty distribution of the P & T axes on the lower right sphere.

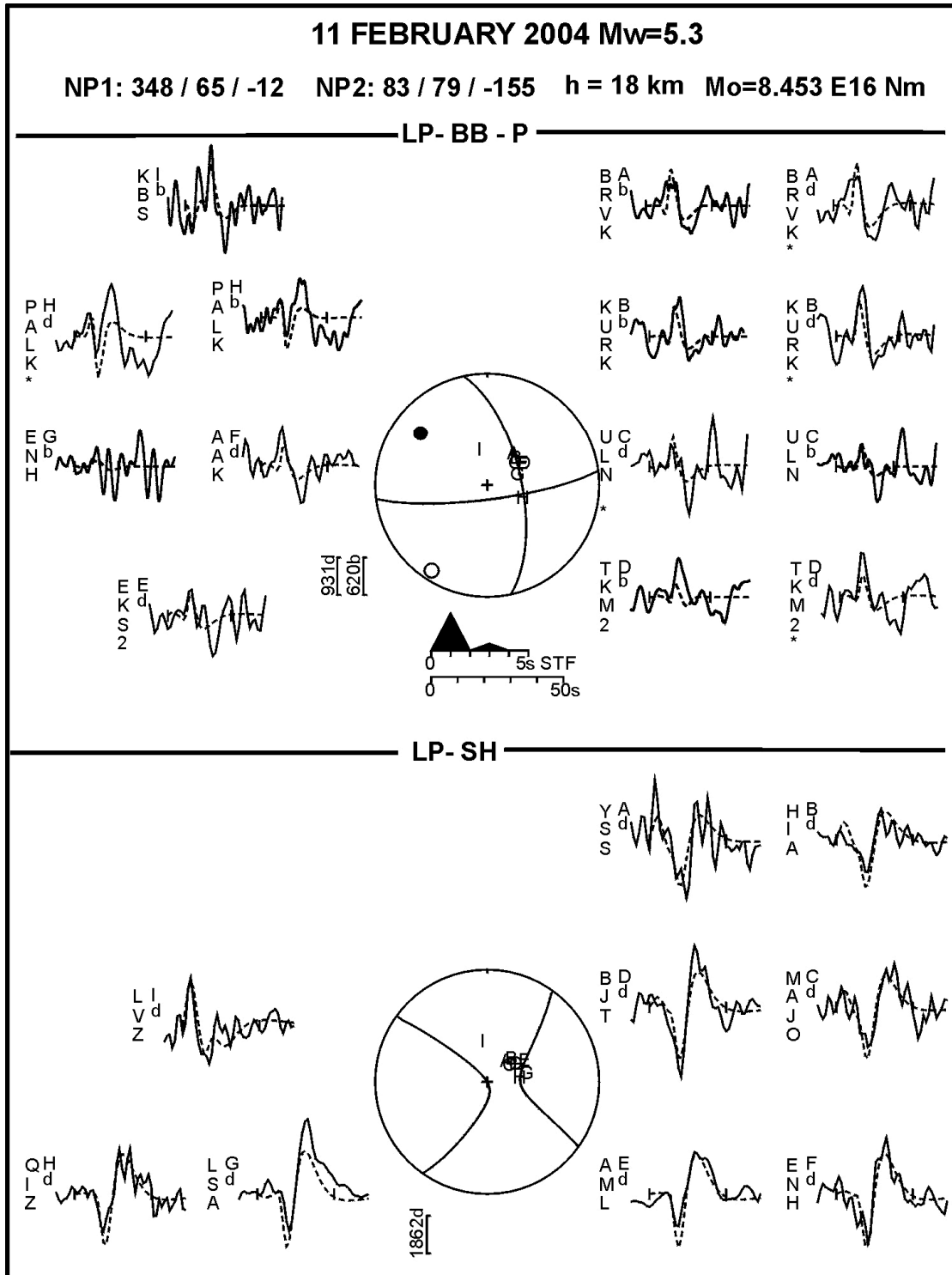


Fig. 5. Waveform inversion fault plane solution of the main shock (by S. Yolsal and T. Taymaz, ITU). The values beneath the event headers show moment magnitude (Mw), strike, dip, rake angles for the nodal planes, depth and seismic moment. The source time function and the time scale used for the waveforms are shown below the P focal spheres. P and T axes within the spheres are marked by solid and open circles, respectively. The parameters are also listed in Table 2.

Table 2. This solution was calculated by using the FPFIT and FPLOT program (Reasenber and Oppenheimer 1985). (see Salamon et al., (2003) for detailed description of the procedure.)

B. Waveform inversion (Fig. 5 and Table 2) by use of teleseismic long-period P- and SH- broad-band P-waveforms, and first motion polarities of P- waves recorded by Global Digital Seismograph Network (GDSN) stations in order to determine the source parameters of the earthquake. The mechanism was calculated by the McCaffrey and Aber's (1988) version of Nabelek's (1984) inversion procedure which minimizes in a weighted least-squares sense, the misfit between the observed and the synthetic seismograms. The shapes and amplitudes of the long period P- and SH-, and broad-band P-waveforms recorded in the distance range of 30 – 90 degrees, for which signal amplitudes were sufficiently large are then compared with the synthetic waveforms (Fig. 5). This iterative inversion procedure continues until a minimum misfit between the observed and the synthetics waveforms is obtained. Seismograms generated by combining direct (P, S) and reflected (pP and sP or sS) phases from a point source embedded in a given velocity structure were weighted according to the azimuthal distribution of stations. Amplitudes were adjusted for geometrical spreading, and for anelastic attenuation using a Futterman's (1962) Q operator, with $t^*=1$ s for P and $t^*= 4$ s for SH. The inversion routine adjusts the strike, dip, rake and depth of the fault, scalar seismic moment and source time function, which is described by a series of overlapping isosceles triangles (Nabelek 1984) whose number and duration are selected. The receiver structure is assumed to be a homogeneous half space.

A depth of 18 km and a seismic moment of 8.5×10^{16} Nm with a simple source time function of about 4s were determined. Synthetic waveforms were calculated for a half space with velocity $V_p=6.5$ km s⁻¹, $V_s=3.7$ km s⁻¹ and $\rho = 2.8$ gr cm⁻³.

C. Another solution (fast CMT) was published by the EMSC a few hours after the event (Fig. 6 and Table 2).

Overall, the three solutions are consistent and show that the sinistral nodal plane strikes about NNW and plunges to the west, and the dextral nodal plane strikes E-W and dips northwards. Though generally this transtensional mechanism is in accordance with the nature of the DST as a leaky transform, the sinistral plane deviates about 30°

anticlockwise off the trend of the transform. Moreover, the dextral plane deviates about 25° clockwise off the general trend of the transversal faults inside the Dead Sea basin. Therefore, it is not clear which structure in the basin triggered this event.

The aftershock sequence seems to cluster west of the main shock and spread in the WNW direction, thus favoring the dextral nodal plane as the actual rupture plane. If so, it reflects the activity of the faults that accommodate the extension parallel to the transform and drives the growth of the basin in a N-S direction (Garfunkel and Ben-Avraham, 2001). However, we are not aware of a specific fault in this location or whether the extension along the basin is accommodated by normal faulting, block rotation or a combined mechanism.

Table 2. Parameters of the main shock mechanism

Parameters	GII	ITU	EMSC
Type of solution	First motion	Wave form Inversion	CMT
NP1 Strike/dip/slip	337/52/-25	348/65/-12	337/51/-35
NP2 Strike/dip/slip	80/70/-140	83/79/-155	91/64/-135
Moment Dyne*cm	-	8.453*10**23	10**23

GII: See Figure 4.

ITU (Istanbul Technical University): See Figure 5.

EMSC: http://www.emsc-csem.org/cgi-bin/ALERT_datafile.sh?S0710&MT; See Figure 6.

The discrepancy between the fault plane solution that reflects the seismotectonics of the deep structure and the surface geology of the Dead Sea basin, emphasizes the inherent difficulties encountered in combining these two layers of data. Our up-to-date knowledge does not enable us to fully understand how the subsurface structures are related to the surface geology. It is interesting to note in this context, the NNW deflection of the

northeastern border fault of the basin as delineated by Garfunkel and Ben-Avraham (2001) that may coincide with the sinistral nodal plane. Whatever the preferred fault plane is and however impressive the ground shaking was, this earthquake was a result of a rupture area of a few km² only, at a depth of about 15 – 20 km. Thus, it does not necessarily display the activity of a primary structural component of the basin.

2.1.3 The aftershock sequence

The main event was followed by a sequence of a few tens of smaller events, the strongest of which occurred a couple of days later and reached a magnitude of 3.7. The activity lasted about half a year, concentrated west of the main shock and distributed in a preferred WNW direction (Table 3 and Fig. 1).

2.1.4 Associated clusters

Seismogenic activity in the Dead Sea Basin was not limited to the 11/2/2004 sequence at that time. Two other series were also recorded within a time span of a year. All three clusters occurred along the eastern margins of the Dead Sea basin.

The first cluster preceded the February shocks about 22 km southwards, opposite 'En Gedi (Fig. 1 and Table 3). The main shock occurred on 31/12/03, reached a local magnitude of 3.7 at a depth of 14 km, and was followed by 4 aftershocks, the last and the strongest of which was triggered simultaneously with the February sequence. The second series may have begun before the February event, about 40 km southwards, near the northern tip of the Lisan peninsula, and culminated after it, on 15/3/2004, with an $M_L=4.3$ main shock (Fig. 1 and Table 3). It is interesting to note that the 7/7/2004 $M_L=4.7$ event occurred 30 km north of the February sequence, in the Jordan Valley, outside the Dead Sea basin (Fig. 1 and Table 3).

The close timing and aerial distribution of these clusters are clear, yet its interacting mechanism, if one exists, is not understood. Possibly, the first three clusters that occurred along the tip of the eastern segment of the transform that comprises the Dead Sea basin, may have induced stresses that triggered the fourth event along the continuation of the transform, outside the basin on the nearby left-stepping segment.

Table 3. Aftershock parameters and other events associated with the 11/2/2004 earthquake. GII catalog: <http://www.gii.co.il/heb/default.html>). Area (old Israeli grid) X:170-220; Y:000-160, time span 1/1/2003-30/9/2004.

Date	Origin Time	Lat	Long	X	Y	Km	ML	mb	Mm	MSK	Type	Region
2003-04-06	10:51:44	31.48	35.42	189.4	98.9	14	2.3	0	0	0		Dead Sea
2003-04-19	03:42:39	31.41	35.52	199.4	90.5	17	2.1	0	0	0		Dead Sea
2003-06-17	17:04:02	31.33	35.41	189.1	82.5	9	2.1	0	0	0		Dead Sea
2003-06-17	18:16:22	31.34	35.39	186.9	83.1	11	2	0	0	0		Dead Sea
2003-07-23	03:03:24	31.21	35.38	186.4	69	13	2.8	0	0	0	PE	Dead Sea
2003-08-15	23:56:21	31.24	35.38	185.8	72	10	2.8	0	2.9	0		Dead Sea
2003-09-17	16:17:31	31.3	35.53	200.3	78.9	21	3	0	2.8	0		Dead Sea
2003-12-31	11:19:16	31.42	35.56	202.8	91.8	5	3.3	0	3.1	0		Dead Sea
2003-12-31	20:44:41	31.5	35.53	200	100.8	14	3.7	4	3.8	3	F	Dead Sea
2003-12-31	20:55:26	31.51	35.52	198.7	101.7	14	2.6	0	0	0		Dead Sea
2003-12-31	21:01:47	31.51	35.52	198.7	101.7	14	2.1	0	0	0		Dead Sea
2003-12-31	21:12:16	31.49	35.51	198	100	13	2.3	0	0	0		Dead Sea
2004-02-11	08:15:03	31.7	35.56	202.3	123	17	5.2	5.1	5.2	6	FS	Dead Sea
2004-02-11	09:09:15	31.73	35.52	198.4	126	15	2.5	0	2.7	0		Dead Sea
2004-02-11	09:21:29	31.78	35.53	199.7	132	18	2.3	0	2.5	0		Dead Sea
2004-02-11	12:33:51	31.7	35.5	197	123.2	15	2.5	0	2.7	0		Dead Sea
2004-02-11	16:17:49	31.71	35.5	197	124.2	14	2.2	0	2.5	0		Dead Sea
2004-02-11	17:31:17	31.72	35.5	196.5	125.4	16	2.6	0	2.8	0		Dead Sea
2004-02-11	19:36:14	31.72	35.51	197.6	124.8	17	2.6	0	2.7	0		Dead Sea
2004-02-12	04:09:41	31.71	35.51	198.1	124.2	16	2.6	0	2.7	0		Dead Sea
2004-02-13	01:23:21	31.71	35.49	195.9	123.9	16	2.6	0	2.8	0		Dead Sea
2004-02-13	05:00:25	31.71	35.49	196.2	124.4	16	2.4	0	2.6	0		Dead Sea
2004-02-13	06:40:14	31.71	35.54	200.4	124.5	14	2.1	0	2.3	0		Dead Sea
2004-02-13	07:02:36	31.7	35.54	200.7	123.1	16	3.7	0	3.6	3	F	Dead Sea
2004-02-13	18:57:21	31.7	35.57	203.1	122.8	16	2.3	0	2.6	0		Dead Sea
2004-02-17	07:22:15	31.51	35.52	198.6	102.1	12	2.9	0	2.8	0		Dead Sea
2004-02-17	07:26:58	30.71	35.26	174.9	12.9	10	2.2	0	0	0		Arava Valley
2004-02-18	05:29:36	31.71	35.53	199.4	124.2	17	2	0	0	0		Dead Sea
2004-02-18	17:42:45	31.64	35.52	198.5	116.8	13	2.1	0	2.2	0		Dead Sea
2004-02-19	01:18:01	31.71	35.5	196.9	124.1	17	2.6	0	2.7	0		Dead Sea
2004-02-19	05:22:07	31.72	35.53	199.8	124.9	16	2.3	0	2.2	0		Dead Sea
2004-02-19	05:47:35	31.72	35.5	196.7	125.1	17	3	0	2.8	0		Dead Sea
2004-02-20	04:46:41	31.72	35.5	196.9	125.2	16	2.8	0	2.8	0		Dead Sea
2004-02-20	05:04:04	31.72	35.5	197.2	125.7	17	2.5	0	2.5	0		Dead Sea
2004-02-24	02:11:32	31.72	35.49	196.2	125.5	17	3.5	0	3.1	3	F	Dead Sea
2004-03-04	21:22:54	31.72	35.46	193.6	125	16	2.1	0	2.4	0		Dead Sea
2004-03-11	02:07:05	31.7	35.51	197.8	123.4	16	2.1	0	2.2	0		Dead Sea
2004-03-15	23:49:56	31.37	35.53	200.3	86.1	13	4.3	4.4	4	3	F	Dead Sea
2004-04-15	17:49:07	31.72	35.49	195.9	124.7	15	2.3	0	2.6	0		Dead Sea
2004-05-13	12:56:29	31.71	35.5	197	124.3	14	2.6	0	2.8	0		Dead Sea
2004-05-25	09:17:52	31.68	35.49	195.8	121.1	15	2.5	0	2.6	0		Dead Sea
2004-05-31	12:35:45	31.72	35.47	194.4	125.3	16	2.8	0	2.9	0		Dead Sea
2004-06-03	13:18:52	32.02	35.49	196	158.6	4	3.2	0	3.2	3	F	E. Shomron
2004-07-05	09:06:39	31.71	35.51	197.5	123.7	16	2.4	0	2.4	0		Dead Sea
2004-07-06	10:11:01	31.42	35.66	211.9	91.9	9	2.3	0	0	0		North Jordan
2004-07-07	14:35:08	31.97	35.55	201.8	153.2	13	4.7	4.8	4.6	4	F	Jordan V.
2004-07-09	12:16:28	31.69	35.57	203.8	121.8	16	3.7	4	3.6	3	F	Dead Sea

2.2 Earthquake induced ground effects

Surface seismogenic ground effects tend to degrade rapidly because of the weather and human activity. It is therefore necessary to document these effects soon after the earthquake while they are still notable.

Immediately after the earthquake and in the days following, teams of the Geological Survey of Israel explored the Dead Sea shorelines, mainly along the Qalya, Darga and Ze'elim coasts, and the southern Jordan River area in search of earthquake-related phenomena. We also interviewed rangers of the local nature reserves and tourist resorts, and local residents who are familiar with the area for any natural effects or unusual phenomena that may relate to the reported earthquake. The findings are presented in Figure 7 and Table 4, and described herein.

2.2.1 Cracks

Cracks were observed along the shore near the Qalya and Darga coasts. They cut through the soft lake sediments and loose alluvial material of the Ze'elim Formation and vary in nature from place to place. They appear sporadically or in clusters; in a wide spectrum of directions; in a linear, arcuate or zigzag pattern; in lengths of a few meters and sometimes up to tens of meters; with a minimal opening and up to a few millimeters offset; as newly formed or reopening of previously existing cracks; and in a spacing of tens of centimeters to a few meters. Each group of cracks seems to be of a homogeneous nature. Overall we distinguished the following types:

- a. Cracks parallel to the sea cliffs that face the waterfront: These are linear cracks, oriented parallel to the seashore and normal to the slope gradient (Photo 1). They seem to indicate low angle gravitational sliding of the soft sediments towards the sea and show the initial stages of slope failure.
- b. Arcuate cracks: These cracks are concave towards the sea and appear at the periphery of developed rotational slumps (Photo 2).
- c. Cracks that strike oblique to the shoreline: Detailed mapping of such cracks was carried out at the Darga coast and is shown in Figure 8. The general trend of these cracks coincides with the orientation of the principal σ_1 stress of the Dead Sea stress field (Eyal and Reches, 1983). These cracks are also sometimes associated

Table 4. List of seismically induced ground effects

No	Category	Type	Locality	N	E	Dist. From epicenter km	E ³ scale	Photo	Remarks
1	Cracks	Parallel	Qalya coast	247.3	629.0	8	VI	1	
2		Arcuate	Qalya coast	247.1	628.5	8	VI	2	
3		Oblique	Darga coast	239.7	608.2	20	VI	3	
4		Reopened	Qalya coast, Darga coast	247.6 239.6	629.3 608.8	8 20	* V	4a 4b	Cracks that formed before the earthquake
5		Superimposed	Darga coast	239.7	608.2	20	* V	5a,b	On mud cracks
6	Slope failure, landslides	Rotational slumps	Qalya coast Hamme En Gedi	247.1 236.4	628.5 591.9	8 35	VI	6a 6b	
7		Collapses	Qalya coast N. Tur-Samar En Shulamit N. Arugot Ze'elim Gully H. Ma'ain, Jordan	247.8 238.5 237.1 235.9 239.2 255	629.5 613.0 597.7 595.8 583.7 615	8 18 30 32 42 9	VI	8 7	Approx. location Unconsolidated talus Unconsolidated talus Approx. location
8		Sporadic rockfalls	N. Qumeran, N. Dawid, N. Bezet	243.4 237.4 220	627.7 597.5 775	11 30 150	IV		In artificial trench In artificial trench
9		Sand boils	Qalya coast	247.5	629.4	8	V	10, 11	Along cracks
10		Water injection	Qalya coast Darga coast	247.5 239.7	629.4 608.2	8 20	V	10	Around boulders
11	Liquefaction	Mud spill	Darga coast	239.7	608.2	20	V	12	
12		Wet sediment	Darga coast	239.7	608.2	20	V	13	
13	Tsunami	Run-up wave, ponds	Qalya coast Darga coast	247.8 239.6	629.7 608.1	9 20	VI	15	
14		Rough sea	Qalya coast	249	628	8	VI	14	
15	Tsunami	Qalya coast	239.6	608.1	20	* VI	16		
16	Water level	Drop/rise	Enot Zuqim Wells	244.2 Table 5	625.9 Table 5	9 Table 5	VI	Table 5	Springs Along the NW coast
17		Sinkholes	Shalem 2 site	237.8	605.9	23	* VI	16, 17	A few sinkholes
18	Radon	Enot Zuqim	242.6	623.5	10.6	* IV	Fig. 11		

19	Dust		NE coast (Jordan)	257	627	5	* V-VI		Approx. location
20	Shaking Palm trees		Darga coast En Gedi	238.4 237.7	611.8 596.1	18 31	IV		
21	Ground wave		NW coast East Jerusalem	248 225	630 633	9 32	?		Approx. location Approx. location
22	Turbidity		NW coast	238	602	25	IV-V	18a,b	Approx. location
23	Unusual water line		Northwestern Dead Sea	250	628	6	?	14	Approx. location
24	Loud noise		Many places				?		

E³ scale: Earthquake environmental effects, INQUA intensity scale (Michetti et al. 2004).

Coordinates - new Israeli grid.

‘*’ Estimated degree of an effect that does not appear in the proposed INQUA scale.

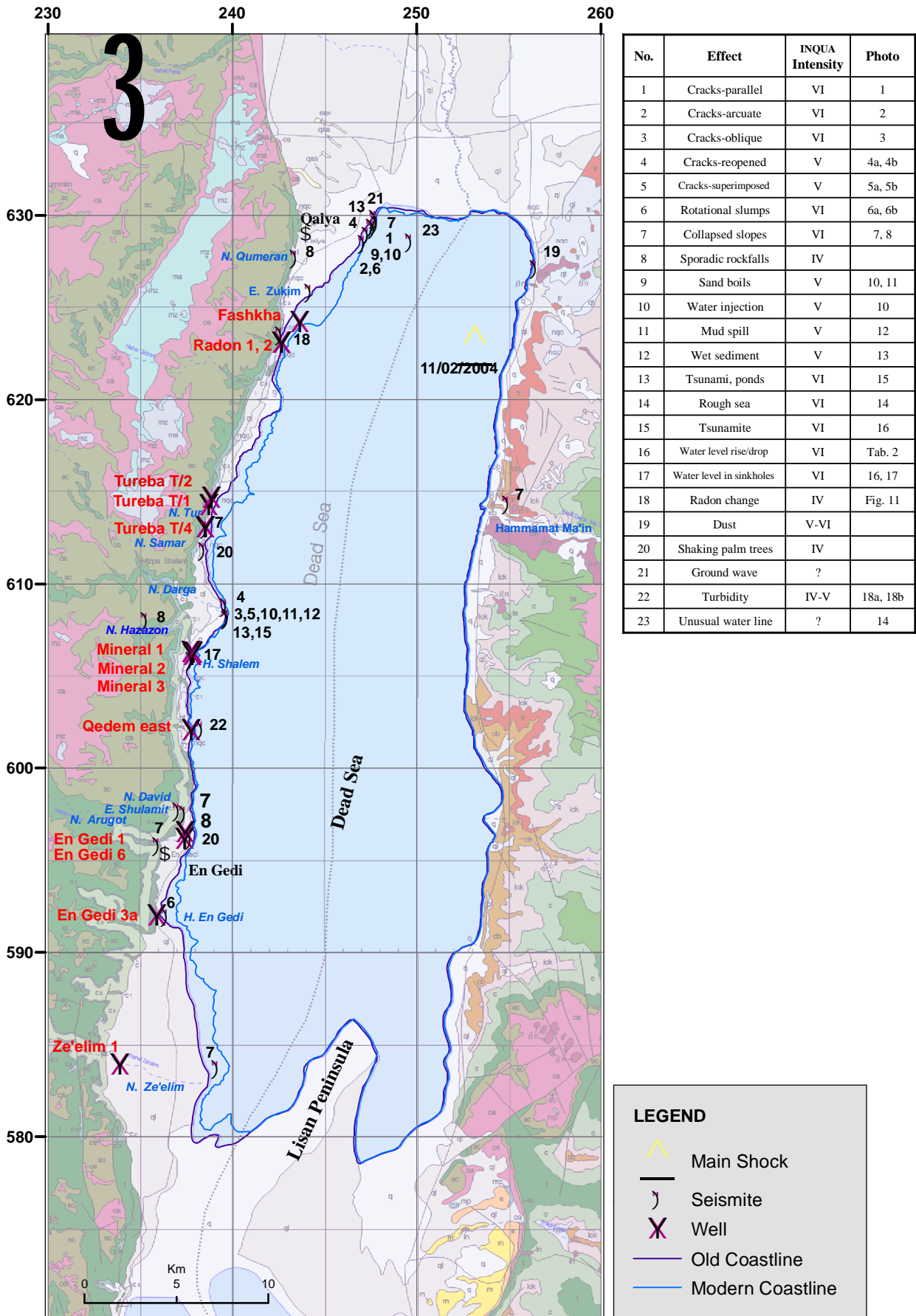


Fig. 7. Location map of the seismogenic effects observed after the 11/2/2004 earthquake along the northwestern Dead Sea shore. See text and Table 4 for a detailed description.

- with localized vertical offset of up to a few centimeters (Photo 3). They seem to reflect differential compaction of loose sediments or of zones that were formerly saturated before the drop of the sea level, probably due to the seismic loading.
- d. Reopened cracks: In many clusters the cracks are linear and parallel. They are oriented parallel, or oblique, or normal to the waterfront - each area in a preferred direction, evenly spaced and with a minimal offset or opening (Photos 4a, 4b). The cracks dissect the lake sediments of the Ze'elim Formation and resemble tectonic jointing. In certain locations, they are closed and partly covered by intact alluvial material. Thus we conclude that they were formed before the earthquake and reopened locally due to ground shaking. Interestingly, some areas along the "modern" coast are covered by long linear stromatolite-like features, spaced a few meters apart (east of Enot Zuqim). Nishri and Nissenbaum (1993) suggested that these are Mn-enriched carbonates that were chemically precipitated in the shallow water near the shore. These incrustations seem to accumulate in superposition with the existing linear cracks. Therefore, we may assume that the formation and the geometry of these sedimentary features were tectonically controlled. These relationships certainly deserve more careful investigation.
 - e. 'Superimposed' cracks: A few seismogenic cracks along the Darga coast were, in part, superimposed on preexisting mud cracks (Photos 5a, 5b) and even on a fractured pebble (Fig. 8). The seismogenic cracks broke the intact sediment below the dried crust of the mud and reopened the mud cracks on the surface. Generally these cracks are linear, but turn zigzag along preexisting mud cracks.

2.2.2 Slope failure

Failure of slopes were observed along the shorelines and few tens of meters inland, between the Qalya and Enot Zuqim coasts, and were associated with open cracks around its margins. We also noted collapses along the steep gully banks of the Enot Zuqim, Hamme En Gedi and N. Ze'elim drainage systems that cut through the newly exposed section of the Ze'elim Formation. Landslides were also reported in the western Ma'ain area, Jordan, on the eastern side of the Dead Sea (R. Hussein, Jordan Times, Thursday, February 12, 2004). Overall a few types of slope failure could be

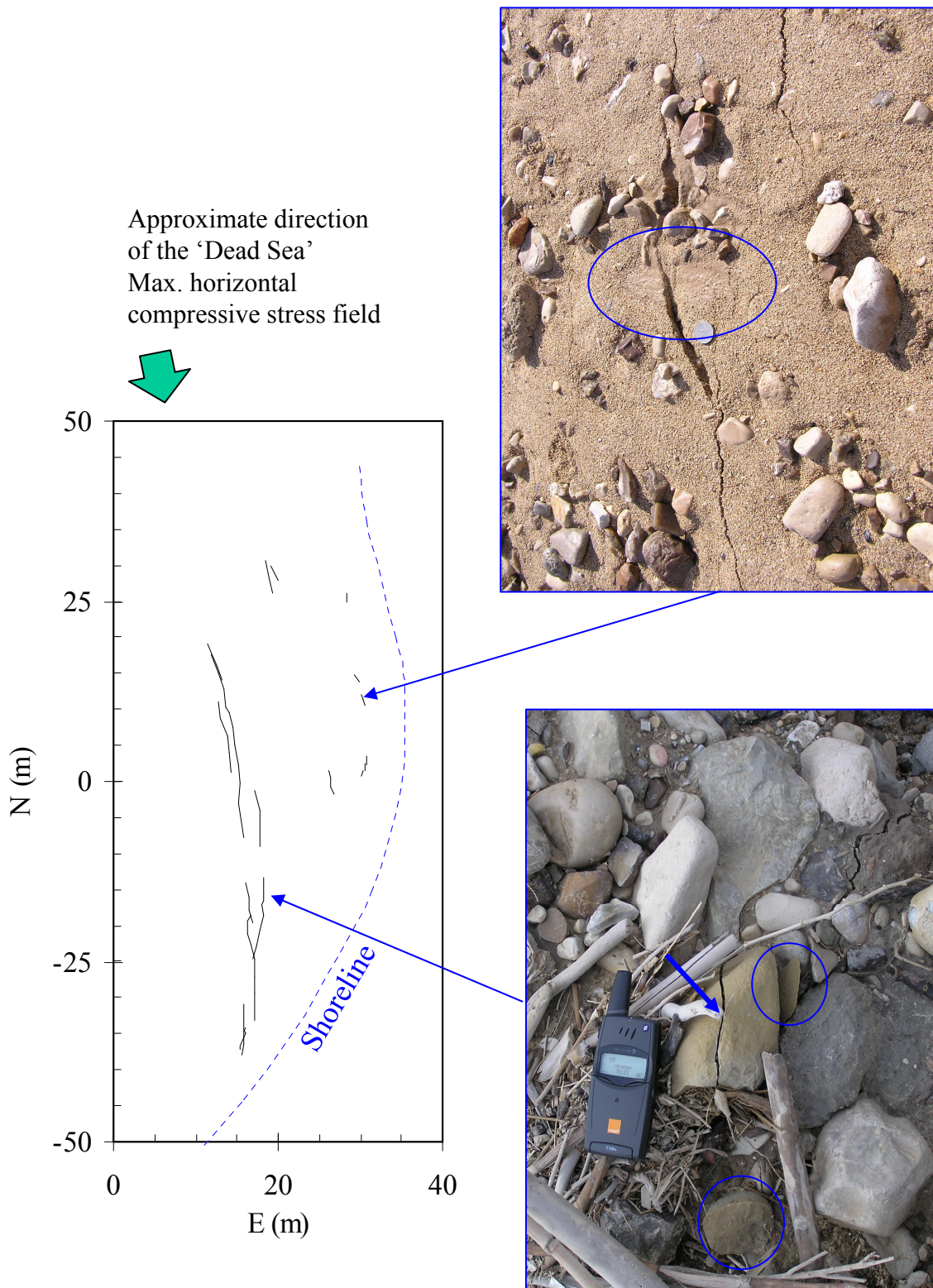


Fig. 8. A detailed map of some seismogenic cracks along the Darga coast. Blue ellipse in the upper photo indicates mud spilled out of the seismogenic crack. Blue circles in the lower photo indicate parts of the pebble that were chipped (possibly during the propagation of the seismogenic crack). North of the map and photos - upwards.

distinguished:

- a. Rotational slumps: Rock masses of the soft unconsolidated Ze'elim section that collapsed towards the sea (Photo 6a). The slumps occurred along the present sea cliffs that rise about 5 m above the sea level and disrupted about a 25 m wide strip of the cliff. A few of the slumps were triggered above saturated layers that discharge ground water. Another slump occurred along an artificial gully bank that drains the Hamme En Gedi hot springs (Photo 6b, courtesy of E. Raz).
- b. Collapses: Fall of rock mass were noted along the newly formed gullies of the N. Ze'elim (Photo 7 and the cover photo) and the Qalya seashore cliffs (Photo 8). Other collapses were reported to occur in a travertine rock near En Shulamit, N. Dawid; in open fissures and a sinkhole that cut through the talus along the foothills near N. Samar and N. Tur (Z. Motsan, pers. comm., 2004); and in hard carbonate (layered and fractured) rocks of the Judea Group at the base of a nearly vertical cliff in N. Arugot (Photo 9).
- c. Sporadic rockfalls: A large boulder fell in N. Hazon (I. Haviv, pers. comm., 2004). Rangers of the Israel Nature and National Parks Protection Authority (INNPPA) reported sporadic rocks falling along slopes composed of poorly cemented alluvial conglomerate in N. Qumeran, N. Dawid and near En Gedi. Rangers of the Soreq Cave, 50 km west of the epicenter, reported low noises of objects rolling on the cave floor, probably of loose rocks and broken speleothems (M. Bar-Matthews, A. Ayalon and E. Kagan, pers. comm., 2004). Another interesting report mentioned sporadic rock falls as far as 150 km north-west of the epicenter, in N. Bezet, Upper Galilee! (D. Wachs, pers. comm., 2004).

2.2.3 Liquefaction

Small sand boils and water ponds (Photos 10, 11) were observed in an artificial trench near the Qalya coast. The trench is a few meters wide and is filled with the loose material. The liquefaction occurred at the bottom of the trench and was associated with open fissures along the inner banks of the trench. These fissures may have formed as a result of minor lateral spreading on top of the liquefied material inside the trench. The sand cones were a few centimeters wide and the water ponds a few tens of centimeters

long. Clay, silty material and foam were associated with the sand boils and the ponds.

Granulometric (dry) analysis of the liquefied material is presented in Figure 9a relative to ranges of grain-size distribution for liquefaction susceptible soils suggested by Tsuchida (1970) and also in Figure 9b in respect to material that was liquefied during the Nuweiba earthquake (Wust, 1997). Originally, the material examined contained 32 wt.% salt and although the profile of the 11/2/2004 material is somewhat different from that of the Nuweiba event, it is still within the boundaries of most liquefiable soils.

Along the Darga coast, we also observed a mud spill along an open crack (Photo 12 and Fig. 8) and wet sediment around sporadic boulders (Photo 13). The mud and the water were probably injected during the earthquake.

2.2.4 Tsunami

Locals at the Qalya coast reported a wave of up to a meter high and a rough sea in the northern part of the Dead Sea soon after the earthquake. A photograph taken a half an hour after the earthquake (courtesy of C. Barghoorn, Qalya) shows a wavy sea near the Qalya shore and also an unusual line in the sea that may have possibly formed just after the earthquake (Photo 14). Residents at En Gedi however, did not notice any unusual wave in the sea.

In the afternoon of that day and the day after, we noticed some water ponds, located a few meters inland along the Qalya and the Darga coasts (Photo 15). In a few places along these coasts, we observed some pebbles lying on top of the washed soft rocks that form the sea shore (Photo 16). Since the sea was nearly flat in the morning and the afternoon of that day, we presume that the ponds and the pebbles (tsunamite?) were emplaced by the run-up wave of the tsunami.

2.2.5 Sinkholes

A drop of about 1 m in the water level in some ponds that fill sinkholes in the Shalem 2 site, south of Mineral Beach, was observed the day after the earthquake. The drop reported by the manager of 'Mineral Beach' resort may have occurred during or immediately after the earthquake and was associated with a loud noise.

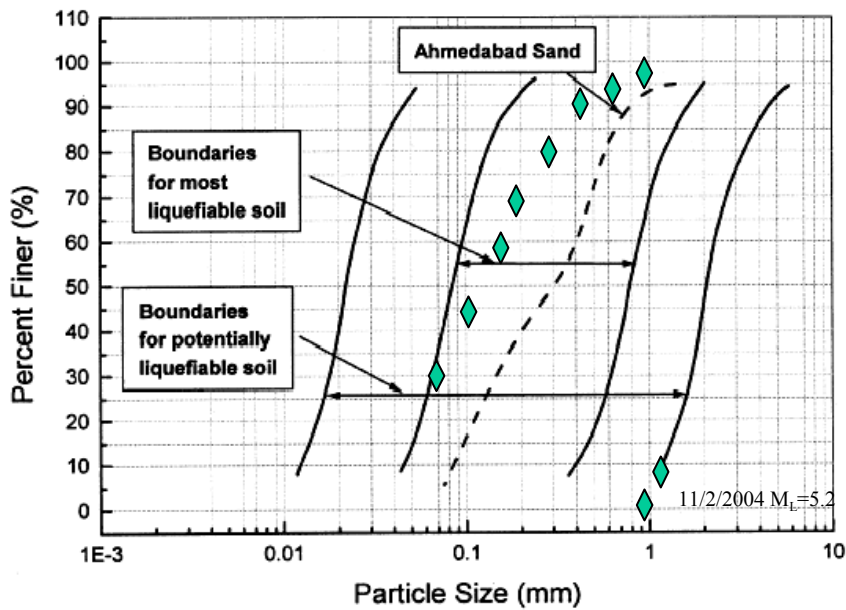


Figure 9a. Granulometric analysis of an ejected material that was liquefied in an artificial trench near the Qalya coast, projected on ranges of grain size distribution for liquefaction-susceptible soils (modified after Tsuchida (1970) and Sitharam et al., (2004).

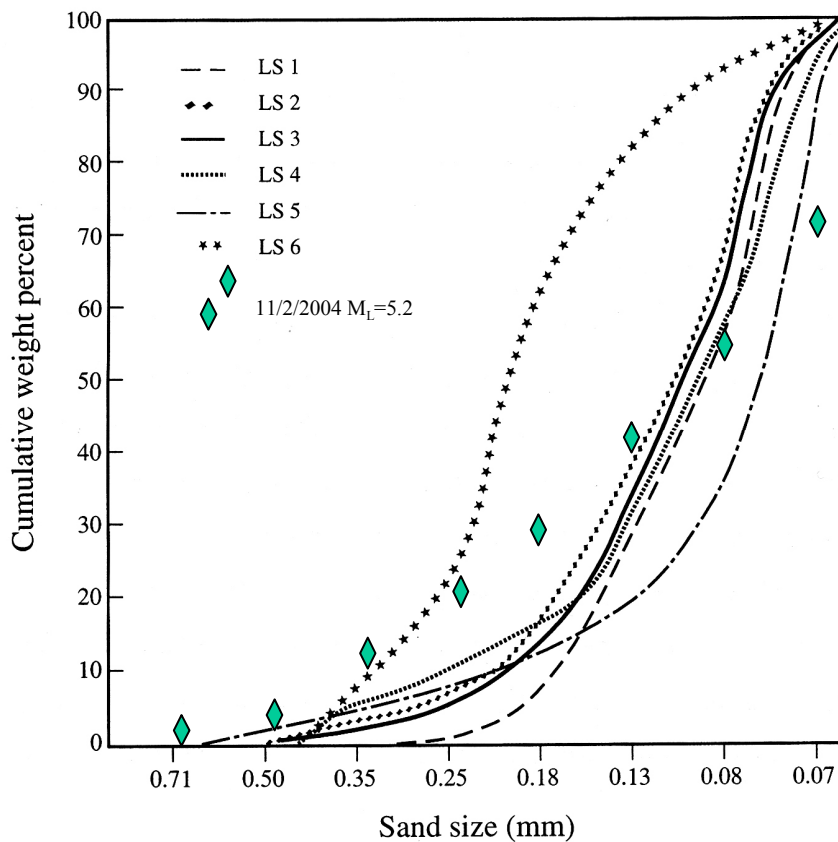


Figure 9b. Granulometric analysis of the material liquefied in the Qalya coast projected on a grain-size distribution of material that was liquefied during the Nuweiba 1995 $M_w=7.1$ earthquake (modified after Wust, 1997).

Field observations suggest that the drop occurred suddenly. Small ponds were left around the upper margins of the sinkhole and above the level of the current pond, indicating that until recently (before the earthquake), they were part of the same water body. Very wet mud found along the slopes of the sinkhole (Photo 17a) also supports this assumption. Stream line features and open cracks that appear in the wet mud at the bottom of the sinkhole (Photo 17b) imply a rapid drop in the water level of the pond. Had the water level dropped gradually and slowly, the upper margins of the sinkhole should have been found dry.

Two new sinkholes were discovered near En Gedi after the earthquake by E. Raz (pers. comm., 2004). However, many new holes developed along the Dead Sea coast during the last few years and it is not clear that these two sinkholes collapsed because of the earthquake.

2.2.6 Water level in wells

A 20-30 cm rise of the water level in some wells along the northwestern coast of the Dead Sea, as well as a small drop in others, was measured (Table 5 and Figures 10a, 10b). The readings were taken the day after the earthquake and were compared with the previous records taken 11 days before the earthquake on 1/2/2004. However, a lack of continuous recording does not enable us to determine the exact timing of the change.

Rangers of the Enot Zuqim (En Fashkha) nature reserve noticed a clear rise of the water level in the ponds and increase of flow in the springs (E. Baruchi, pers. comm., 2004)

Flexer and Guttman (2004) reported a sharp rise of 4.5 m in the water level of the Ravaya 6 well, 45 minutes before the earthquake. The water level kept rising another 1.2 m after the event and then dropped down to its original level. The well is located in the rift valley, 75 km north of the epicenter and the pressure head of the Cenomanian-Turonian aquifer of the region is continuously monitored in it. Such a precursory water level anomaly is exceptionally high, even if associated with strong earthquakes (Roeloffs, 1988) and therefore should be verified carefully.

Table 5. Change of water level in wells along the northwestern coast of the Dead Sea

Well	Water level change (cm)	Coordinates New Israeli Grid	Distance from epicenter (km)	Remarks
Fashkha	- 6	243658/624226	10	Shallow drill
Radon 1**	+ 25	242660/623120*	11	-
Radon 2**	+ 36	242660/623120*	11	-
Tureiba T/1	No change	238720/614290*	17	Upper aquifer
Tureiba T/2	No change	238860/614680*	17	Upper aquifer
Tureiba T/4	- 5	238530/613090*	18	Upper aquifer
Tureiba T/4	+ 12	238530/613090*	18	Lower aquifer
Mineral 1	+ 28	237739/606320	23	-
Mineral 2	+ 23	237886/606291	23	-
Mineral 3	No change	237810/606169	23	-
Qedem east	+ 15	237710/602056	26	-
En Gedi 1	+ 6	237441/596557	31	-
En Gedi 3a	+ 11	235900/592000*	35	-
En Gedi 6	+ 4	237396/596199	31	-
Ze'elim 1	- 6	233892/583929*	43	-

* Estimated coordinates

** Also site of the 17W Enot Zuqim Gamma detectors (radon concentration)

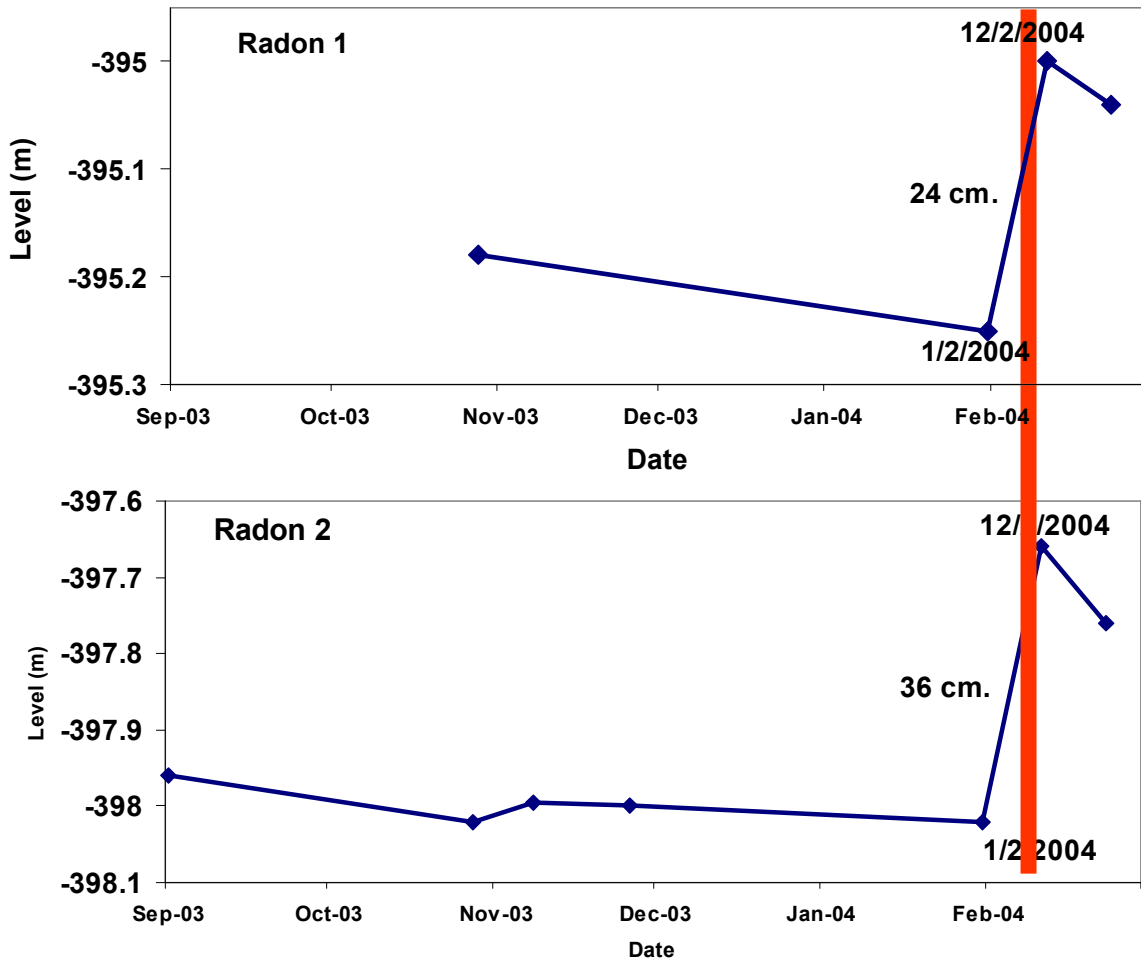


Fig. 10a. Change of water level (blue profile) in the Radon 1 and 2 wells associated with the 11/2/2004 earthquake (red bar).

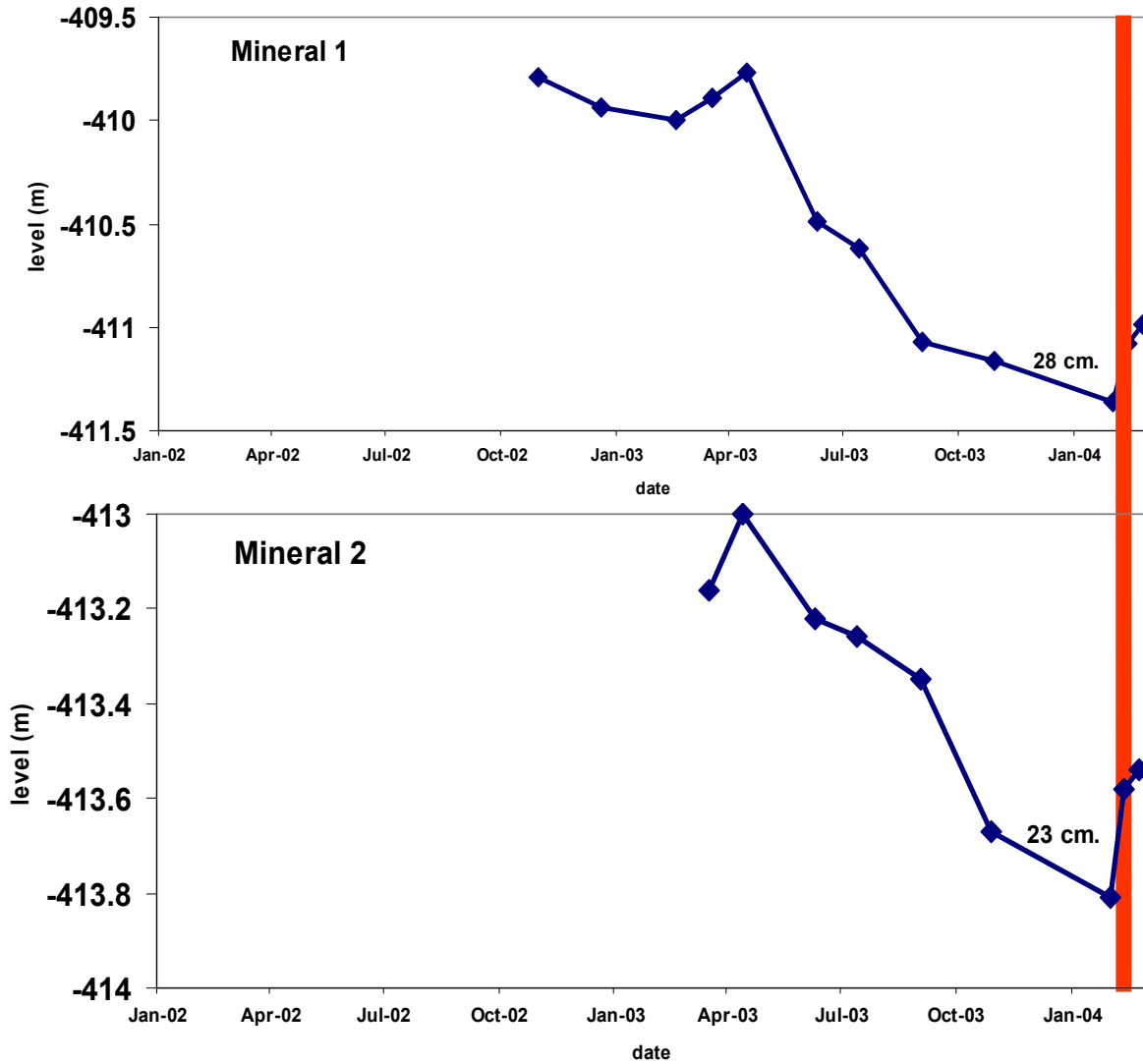


Fig. 10b. Change of water level (blue profile) in the Mineral 1 and 2 wells associated with the 11/2/2004 earthquake (red bar).

2.2.7 Radon flux

A sudden break in the daily pattern of the radon concentration was registered by two of the Enot Zuqim monitors, 10-14 hours before the earthquake (Fig. 11). The continuous monitoring was carried out by two Gamma detectors at site 17W, near the Radon 1, 2 wells (Table 5), in 15 minutes registration intervals (Steinitz et al., 2003). The signal displayed in Figure 11 presents the residual of the 25 hour sliding average and it appears that the typical daily pattern is disrupted 10-14 hours prior to the earthquake. These phenomena are under further investigation.

2.2.8 Other natural effects

Dust was seen (by Enot Zuqim rangers) along the northeastern coast of the Dead Sea immediately after the earthquake. The dust could have possibly risen because of landslides.

Noise: Many people both near and far away from the epicenter, reported a loud noise associated with ground shaking.

Wavy motion of the ground: A few people saw a wavy motion of the surface of the ground during the earthquake.

Shaking palm trees along the Darga coast and also in En Gedi were reported by the planters.

Long distance shaking: People in the NW Galilee, as far as 160 km NNW of the epicenter, were frightened (Kibbutz Elon), ran outside (Arab-el-Aramsha village) and reported sporadic rockfalls in N. Bezet (D. Wachs, pers. comm., 2004). These could be measured as degree V in the MSK and IV in the INQUA intensity scales, higher than is expected for that unusually long distance.

2.2.9 Doubtful effects

Some phenomena attracted our attention as seismogenic effects, although they appear in the area from time to time not necessarily associated with an earthquake and we could not rule out the possibility that they were not induced in another manner. Nevertheless, these effects are noted because it is reasonable to assume that they might have been

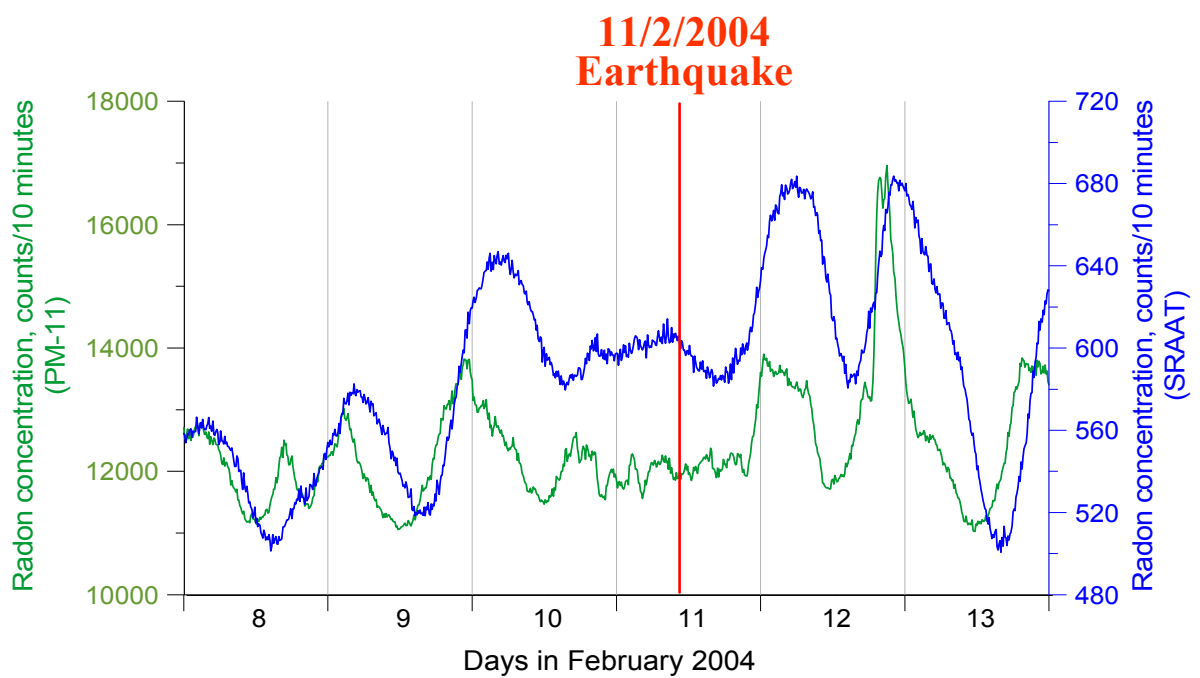


Fig. 11. The daily pattern of the radon concentration a few day before and after the earthquake. The signal displayed here is the residual of the 25 hour sliding average and it appears that the typical daily pattern is disrupted 10-14 hours prior to the earthquake.

induced by the earthquake.

Small turbidities were seen along the waterfront between the En Gedi and the Darga coasts (Photos 18a, b), five hours after the event. They seemed like clouds of suspended material in the water. However, turbidities in the Dead Sea appear from time to time, e.g., during floods and winter flow of the Jordan River (Raz, 1993). If triggered by a seismic shock, these seismites could have formed by the shaking of loose unconsolidated sediment at the bottom of the sea, by local submarine landslides and also by wash of alluvial material from the coast into the sea by the returning tsunami wave.

An unusual line in the sea was photographed (Photo 14) near the Qalya shore, about half an hour after the earthquake. This odd line was reported to move very slowly northwards. However, such lines have been seen previously, not necessarily associated with an earthquake (C. Barghoom, pers. comm., 2004). Raz (1993) presents a very similar front line that was formed by the large inflow of the Jordan River water into the Dead Sea during the 1992 rainy winter.

Since the water column of the Dead Sea is not presently layered, this line could not be considered as 'whitening' (crystallization of gypsum) triggered by seismogenic mixing of the upper water layers of the sea. At this stage we are not certain of the origin of this line.

3 DISCUSSION

Most of the findings were observed, photographed and documented a few hours and up to a few days after the earthquake. A number of the effects were directly observed during the earthquake or immediately after it: loud noise, tsunami and a rough sea, dust, shaking of palm trees, wavy motion of the ground, collapse of sporadic boulders and the unusual water line.

Some of the effects occur regularly in the region, as part of the ongoing degradational processes and we had to resolve which of them represent seismogenic effects. Fortunately, a storm hit the region a week before the earthquake (5/2/2004) and left clear imprints of raindrops on the ground and traces of floods along the N. Ze'elim gullies. We therefore were able to single out the ground effects that occurred after the storm. Still there may be a slight possibility that some of the effects occurred spontaneously a few days before or a few hours after the earthquake.

3.1 Failure effects and vulnerability of the young formations

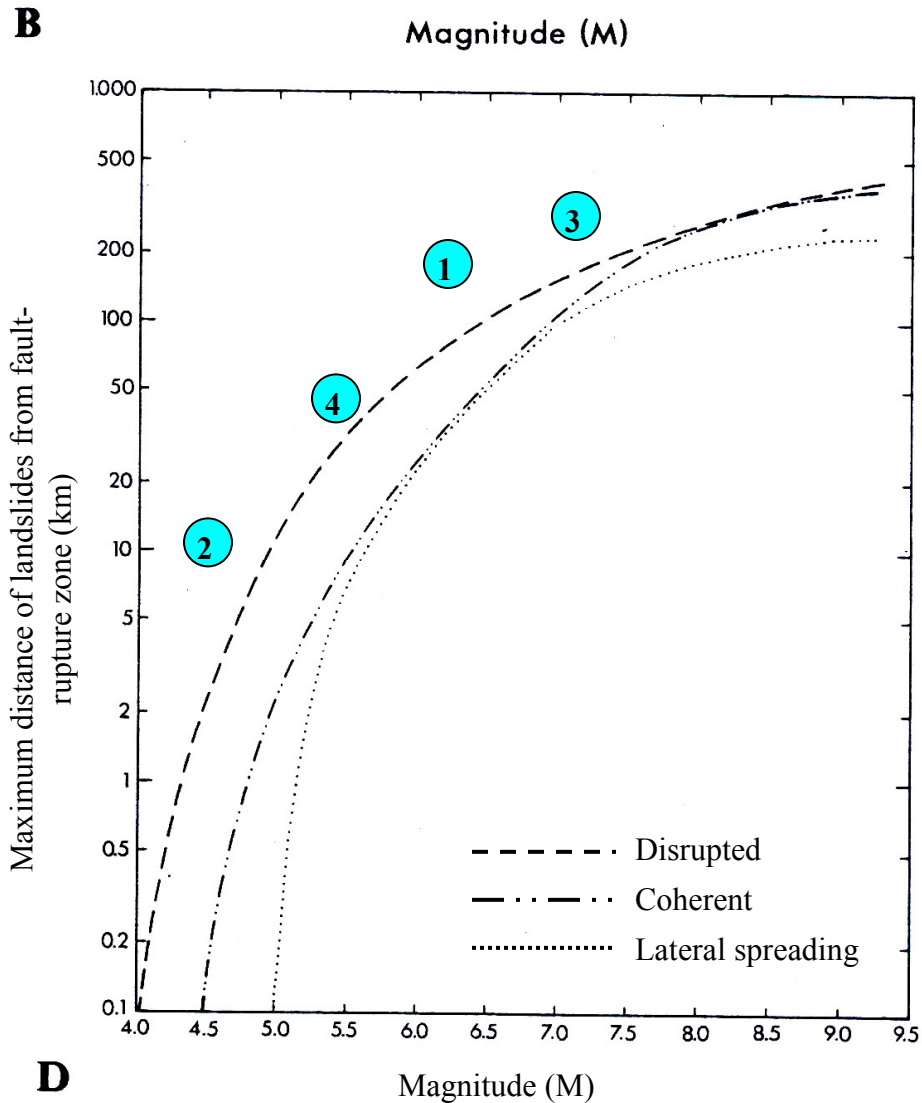
Most of the failure events occurred within a range of 40 km from the epicenter and mainly affected the exposed sediments of the Ze'elim Formation. Cracks and landslides that were observed after the earthquake also occur in the region because of the erosional processes already prevailing such as flooding, sea level changes and weather. These are considered as secondary effects (Appendix 2, after Michetti et al., 2004) and occur where conditions of equilibrium are unstable. Primary effects however, such as surface rupture and liquefaction in natural ground that occur only during a strong earthquake, were not observed.

The lithology and depositional history of the Ze'elim Formation are of critical importance in determining its reaction to seismic forces. The rocks comprising this unit are soft, unconsolidated, have a high water content, and formed during the Holocene. Thus, geotechnically this unit is very weak.

Failure in the Lisan Formation caused by the present event was not observed. However, previous moderate events that hit the region did induce ground failure in the Lisan rocks (Arieh et al., 1977, 1980, 1982). However, it is important to note that the Holocene deposits were not as widely exposed at that time as nowadays. Therefore, the Lisan Formation should be considered as the second weakest unit in the region.

Worldwide experience shows an empirical relationship between ground failure and distance from the earthquake epicenter. Keefer (1984) correlated the maximum distance of earthquake induced landslides with respect to the magnitude of a given earthquake. Projection of our observations, as well as data from other previous events in Israel, onto Keefer's findings shows that it is more sensitive (Fig. 12). Wust and Wachs (2000) attributed the sensitivity in northern Israel to asymmetrical dispersion of seismic energy and further enhancement of that energy due to channeling along the Dead Sea Rift structure. The sensitivity of the Dead Sea region, however, is attributed to the weak geotechnical nature of the Ze'elim and Lisan formations.

Projection of the 11/2/2004 liquefaction event on the empirical relationships between magnitude and distance for liquefaction as given by Galli (2000) shows that it coincides with the global experience (Fig. 13). Although it reflects the behavior of an artificial ground surface rather than the natural ground conditions, it still emphasizes the



1. Dead Sea, 1927 (Wust & Wachs, 2000)
2. Ma'agan, 1973 (Arieh et al., 1977)
3. Nuweiba, 1995 (Weinberger, pers. comm., 2004)
4. N. Ze'elim, Dead Sea 2004 (this work)

Fig. 12. Moment-magnitude versus maximum distance for slope failure according to Keefer (1984). Superposition of the occurrences of slope failure in Israel, including failure in N. Ze'elim during the 11/2/2004 event (circle 1), seems to indicate that this region is more vulnerable.

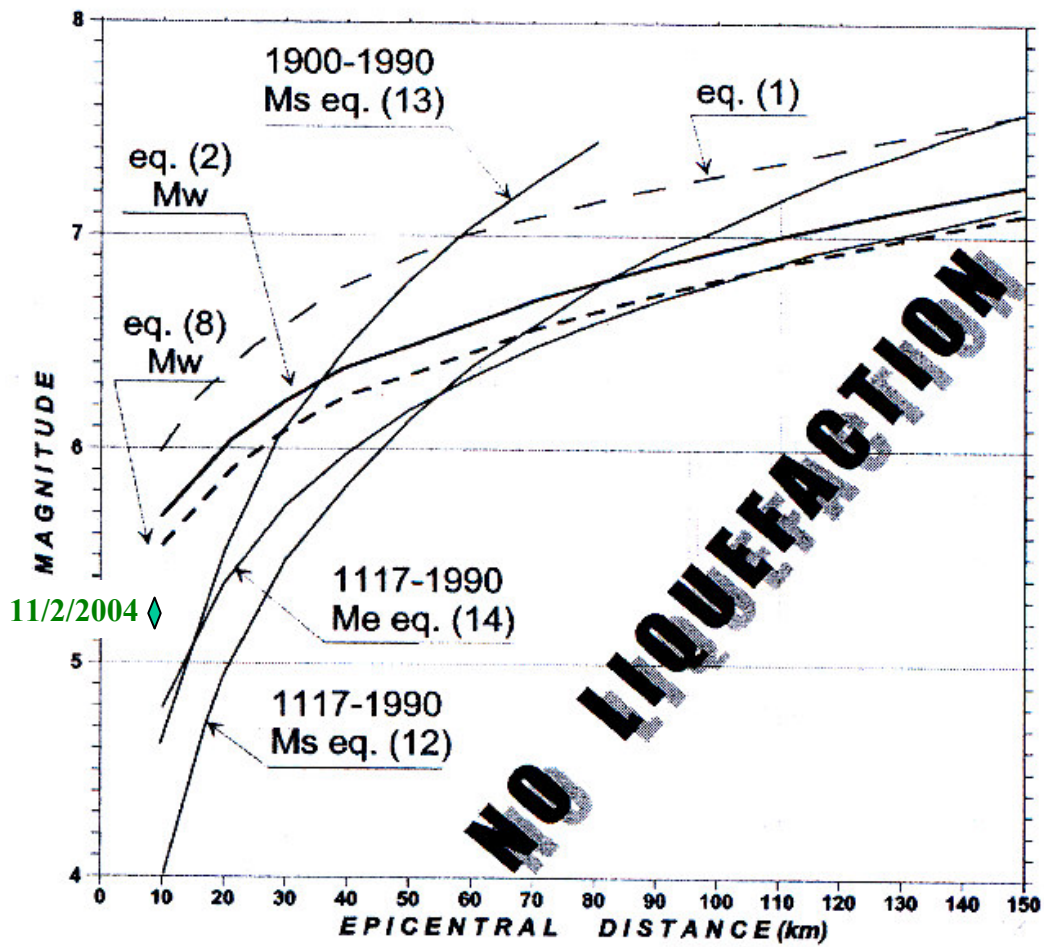


Fig. 13. The 11/2/2004 liquefaction event is superimposed on the empirical relationships between magnitude and distance for liquefaction as given by Galli (2000).

vulnerability of man-made structures to seismic loading if not properly designed.

Arieh et al. (1977) already realized that “unconsolidated ground produces an exaggerated response even to a small earthquake”. Our observations support their conclusion and emphasize the vulnerability of the young deposits within the Dead Sea rift to failure even during a moderate shaking. These are the Late Pleistocene Lisan sediments that are marked ‘ql’ on the geological map of the region (Sneh et al., 1998) and the Holocene Ze’elim Formation that is marked ‘q’ on that map and is also exposed in the area between the old and the modern coastlines (Figs. 7, 14).

3.2 Earthquake intensities - the INQUA EEE scale

The newly proposed “INQUA EEE scale” (E^3 scale) (Michetti et al., 2004) formalizes “Earthquake Environmental Effects” in an intensity scale and thus enables us to evaluate the strength of the earthquake in terms of its associated natural seismogenic effects (Appendices 1, 2, 3). The E^3 scale can also be correlated with the commonly used macroseismic intensity scales (e.g., MCS, MSK, MM) that are based on subjective reports of people and on damage to man-made structures (Michetti et al., 2004).

We attributed E^3 intensity degree to each of the observed effects according to the newly proposed scale (Table 4) and constructed an E^3 intensity map of the 11/2/2004 event (Fig. 14). The maximal degree is found to be VI and most of its occurrences are in the Ze’elim sediments, as far as 40 km away from the epicenter. Effects observed within the Lisan outcrops were limited only to change of water level in wells. Only one effect was found outside the range of the young sediments – collapse at the base of a very steep cliff of the Judea Group in N. Arugot (Photo 9). The low degrees (I-III) of the E^3 scale are difficult to resolve because, by definition, “extremely rare occurrences of small effects... or variations” (Appendix 1) are needed to contour these isoseismals.

Therefore, it seems that the spread of the environmental effects mainly follows the areal distribution of the Ze’elim Formation rather than a uniform distance-dependent distribution around the epicenter. Thus the E^3 intensity map is actually delineates the most vulnerable unit in the region.

Preliminary analysis of the macroseismic data according to the MSK scale (GII data)

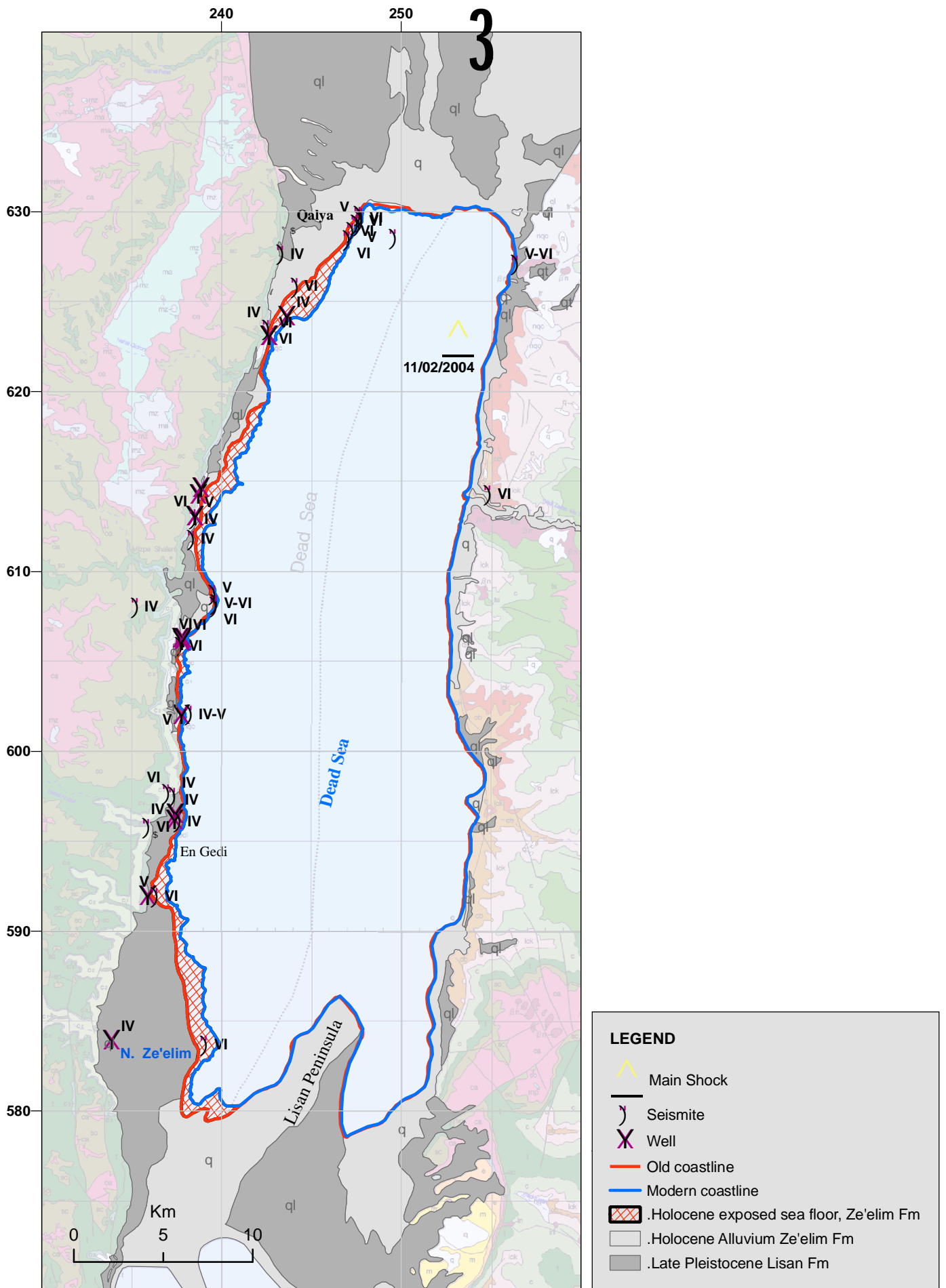


Fig. 14. Inqua EEE intensity map of the 11/2/2004 earthquake, superimposed on the geological map of the region (Sneh et al., 1998). See text and Table 4 for a detailed description.

shows that the maximal degree is V–VI, in accordance with the maximal degree of the INQUA scale. However the MSK high degrees appear not only near the Dead Sea but also further away, as far as Bet Shemesh, 50 km westwards, where people reported fallen objects and a few cracks in buildings, and in Nablus, 60 km NW of the epicenter (Al-Dabbeek et al., 2004). It is interesting to note the high MSK degrees in the NW Galilee that were mapped after the April 1979 Dead Sea earthquake (Arieh et al., 1980, Fig. 3), accord with the long distance shaking reported in the 11/2/2004 earthquake. This may point to an unusual amplification effect in this area or direction from the epicenter.

Overall, we expect good agreement between the maximal degrees of the E^3 and the MSK scales in regard with the 11/2/2004 event, but a considerable difference in its aerial distribution.

3.3 Post earthquake investigations

Most of the failure effects of the 11/2/2004 event are typical of ongoing degradation processes in the region and tend to fade away within days. If not documented immediately, these effects become impossible to identify and differentiate. Therefore it is important to detect and monitor these features (Appendix 3) immediately after the earthquake. Here we were fortunate in that a rainstorm occurred one week before the earthquake. It set off the ‘degradation clock’ and allowed us to distinguish between failure effects that occurred before the rainstorm and the seismogenic effects that occurred after. This may not necessarily be the case in the future; hence the fieldwork should always be carried out as early on as possible.

4 CONCLUSIONS

The 11/2/2004, $M_L=5.2$ northeastern Dead Sea earthquake induced a wide spectrum of natural effects and gave us an exceptional opportunity for systematic documentation. Most of the natural seismogenic effects in Israel were found along the northwestern coastal area of the Dead Sea shoreline, within a range of 40 km from the epicenter.

The failure effects include cracks originating from gravitational movements, differential compaction and reopening of existing joints, landslides along the cliffs that face the waterfront, collapses along gully banks that cut through the soft Holocene deposits, and fall of sporadic rocks in steep unconsolidated slopes. All these phenomena seem to occur regularly in this region and the earthquake accelerated these ongoing degradation processes. Other failures were mud spill along open fractures and liquefaction in an artificial trench.

Additional effects which were observed soon after the earthquake in the northern Dead Sea were a tsunami up to a meter high and a rough sea, a rise in water level of up to 30 cm in some wells along the northwestern Dead Sea shoreline and a drop of a few centimeters in a few others, a noticeable increase in flow from the Enot Zuqim springs, a sudden drop of about a meter in the water level in a few sinkholes of the Shalem 2 site, water injection around sporadic boulders, and a disruption in the daily pattern of the radon concentration in two of the Enot Zuqim monitors 10-14 hours before the earthquake. Dust, loud noise, wavy motion of the ground and shaking of palm trees were also observed.

The failure effects most severely affected the soft Holocene deposits of the Ze'elim Formation, mainly at the unstable waterfront cliffs and gully banks. This indicates that geotechnically, the Ze'elim Formation is the weakest unit in the region and therefore is extremely vulnerable to failure, even by a seismic load of a moderate earthquake. This is in accordance with Arieh et al. (1982), who concluded after the 23/4/1979 earthquake that "Therefore, an evaluation of seismic risk in Israel should always include a consideration of local ground conditions".

A maximal degree of VI is reached according to the newly proposed INQUA E^3 intensity scale that is based on seismogenic ground effects. We expect this to correlate

with the maximal degree of the macroseismic MSK scale of damage to man-made structures, though the aerial spread of the effects of the two scales may differ considerably.

The seismogenic effects tend to fade away within days after the earthquake and some of them resemble morphologies of natural failures that already exist in the region. Therefore, seismogenic ground effects should be immediately detected and monitored before they can no longer be distinguished.

5 ACKNOWLEDGMENTS

We thank D. Wachs, E. Raz, M. Stein, I. Haviv and Z. Motsan for sharing with us their wide knowledge and experience. B. Cohen and N. Shragai helped us with the drawings and B. Katz and R. Bogoch with editing the text.

6 REFERENCES

- Al-Dabbeek, J., Al-Kelani, R., Dwaikat, M. and Arafat, A., 2004. Dead Sea earthquake of 11 February, Mb 5.1, A preliminary report. http://www.relemr-merc.org/ESSE/Jalal_11-02-04Earthq.htm.
- Amit, R., Zilberman, E., Porat, N. and Enzel, Y., 1999. Relief inversion in the Avrona Playa as evidence of large-magnitude historical earthquakes, Southern Arava Valley, Dead Sea Rift. *Quatern. Res.*, 52, 76-91.
- Amiran, D. H. K., Arieh, E. and Turcotte, T., 1994. Earthquakes in Israel and adjacent areas: Macroseismic observations since 100 B.C.E. *Isr. Explor. J.*, 44 (3-4), 260-305.
- Arieh, E., Peled, U. and Kafri, U., 1977. The Jordan valley earthquake of September 2, 1973. *Isr. J. Earth Sci.*, 26, 112-118.
- Arieh, E., Peled, U. and Rotstein, Y., 1980. The Dead Sea earthquake of April 23, 1979. *Inst. Petrol. Res. Geophys. (IRPG)*, SL/567/79 - (4).
- Arieh, E., Rotstein, Y. and Peled, U., 1982. The Dead Sea earthquake of 23 April 1979. *Seismol. Soc. Am., Bull.*, 72, 1627-1634.
- Avni, R. 1999. The 1927 Jericho earthquake, comprehensive macroseismic analysis based on contemporary sources (in Hebrew, Engl. Abstr.). Ph.D. Thesis, Ben-Gurion Univ. of the Negev.
- Ben-Menahem, A., Nur, A. and Vered, M., 1976. Tectonics, seismicity and structure of the Afro-Euroasian junction -The breaking of an incoherent plate. *Phys. Earth Planet. Inter.*, 12, 1-50.
- Bentor, Y. K., 1989. Geological events in the Bible. *Terra Nova*, 1 (4), 326-338.
- El-Isa, Z. H. and Mustafa, H., 1986. Earthquake deformations in the Lisan deposits and seismotectonic implications. *Geophys. J. Royal Ast. Soc.*, 86, 413-424.
- Eyal, Y. and Reches, Z., 1983. Tectonic analysis of the Dead Sea rift region since the Late-Cretaceous based on mesostructures. *Tectonics*, 2 (2), 167-185.
- Feldman, L., Hofstetter, R., Gitterman, Y., Zaslavsky, Y., Pinsky, V. and Peled, U., 2004. The northern Dead Sea strong earthquake on 11/2/04. *Isr. Geol. Soc., Annu. Meet., Abstr.*, p. 26.
- Flexer, A. and Guttman, Y., 2004. Water level change in a well - A precursor to the earthquake of February 11th, 2004. *Isr. Geol. Soc., Annu. Meet., Abstr.*, p. 28.

- Futterman, W. I., 1962. Dispersive body waves. *J. Geophys. Res.*, 67 B12, 5279-5291.
- Galli, P., 2000. New empirical relationships between magnitude and distance for liquefaction. *Tectonophysics*, 324, 169-187.
- Garfunkel, Z., 1981. Internal structure of the Dead Sea leaky transform (rift) in relation to plate kinematics. *Tectonophysics*, 80 (1-2), 81-108.
- Garfunkel, Z., Ben-Avraham, Z., 2001. Basins along the Dead Sea transform. In: P. A. Ziegler, W. Cavazza, A. H. F. Robertson & S. Crasquin-Soleau, (eds.), *Peri-Tethys Memoir 6: Peri-Tethyan Rift/Wrench Basins and passive margins*, Paris, Mem. du Musee Nat. d'Hist. Natur., 186, 607-627.
- Geophysical Institute of Israel (GII), 1996. *Seismological Bulletin 1900-1995*. Seismology Division, <http://www.gii.co.il/>
- Institute for Petroleum Research and Geophysics (IPRG), 1982-1993. *Earthquakes in and around Israel*. Seismological Division, Holon, Israel, *Seismological Bulletins*, 1-12.
- International Seismological Centre (ISC), 1964-1993. *Bulletin*, Edinburgh.
- International Seismological Centre (ISC), 1991. *Bulletin Data Base*, FAISE Retrieval Software for the Hypocenter Associated Data CD-ROM, USGS/NEIC.
- International Seismological Centre (ISC), 2000. *Database selection*.
http://www.isc.ac.uk/Bulletin/index_db.html
- International Seismological Summary (ISS), 1918-1963. *Bulletin*, Berkshire, U.K.
- Keefer, D. K., 1984. Landslides caused by earthquakes. *Bull. Geol. Soc. Am.*, 95, 406-421.
- Ken-Tor, R., Agnon, A., Enzel, Y., Stein, M., Marco, S. and Negendank, J. F. W., 2001. High-resolution geological record of historic earthquakes in the Dead Sea basin. *J. Geophys. Res.*, 106 (B2), 2221-2234.
- Klinger, Y., Avouac, J. P., Abou Karaki, N., Dorbath, L., Bourles, D. and Reys, J. L., 2000a. Slip rate on the Dead Sea transform in northern Araba valley (Jordan). *Geophys. J. Int.*, 142, 755-768.
- Klinger, Y., Avouac, J. P., Dorbath, L., Abou Karaki, N., Tisnerat, N., 2000b. Seismic behaviour of the Dead Sea fault along Araba valley, Jordan. *Geophys. J. Int.*, 142, 769-782.
- McCaffrey, R. ve Abers, G., 1988. SYN3: A program for inversion teleseismic body

- waveforms on microcomputers. Hanscomb Air Force Geophysics Laboratory, Tech. Rep., AFGI-TR-88-0099, 50 p.
- Marco, S. and Agnon, A., 1995. Prehistoric earthquake deformations near Masada, Dead Sea graben. *Geology*, 23 (8), 695-698.
- Marco, S., Agnon, A., Ellenblum, R., Eidelman, A., Basson, U. and Boas, A., 1997. 817-year-old walls offset sinistrally 2.1 m by the Dead Sea transform. *J. Geodyn.*, 24, 11-20.
- Michetti, A. M., Esposito, E., Gurpinar, A., Mohammadioun, B., Mohammadioun, J., Porfido, S., Rogozhin, E., Serva, L., Tatevossian, R., Vittori, E., Audemard, F., Comerci, V., Marco, S., McCalpin, J. and Morner, N. A., 2004. The INQUA Scale - An innovative approach for assessing earthquake intensities based on seismically-induced ground effects in natural environment. Special Paper, Working group under the INQUA Subcommittee on Paleoseismicity, Mem. Descr. Carta Geol. Italia, Vol. LXVII, 118 p.
- Nabelek, J. L., 1984. Determination of earthquake source parameters from inversion of body waves. Ph.D. Thesis, M.I.T., U.S.A.
- Niemi, T. M., 1997. Preliminary estimate of paleoearthquakes along the northern Wadi Araba Fault, Dead Sea Transform, Jordan. *GSA Abstracts with Programs*, v. 29, No. 6, A-131.
- Niemi, T. M. and Ben-Avraham, Z., 1994. Evidence for Jericho earthquakes from slumped sediments of the Jordan River delta in the Dead Sea. *Geology*, 22, 395-398.
- Nishri, A. and Nissenbaum, A. 1993. Formation of manganese oxyhydroxides on the Dead Sea coast by alteration of Mn-enriched carbonates. *Hydrobiologia*, 267, 61-73.
- Nur, A., 1991. And the walls came tumbling down. *New Scientist*, 6, 45-48.
- Raz, E., 1993. *The Dead Sea Book*. Nature Reserves Authority, 216 p. (in Hebrew).
- Reasenber, P. and Oppenheimer, D., 1985. FPFIT, FPLOT and FPPAGE: Fortran computer programs for calculating and displaying earthquake fault-plane solutions. USGS, Open-file report 85-739.
- Reches, Z., and Hoexter, D. F., 1981. Holocene seismic activity in the Dead Sea area. *Tectonophysics*, 80, 235-254.
- Roeloffs, E. A., 1988. Hydrologic precursors to earthquakes: A review. *Pure Appl.*

- Geophys. (PAGEPH), 126 (2-4), 177-209.
- Rotstein, Y., 1987. Gaussian probability estimate for large earthquake occurrence in the Jordan Valley, Dead Sea rift. *Tectonophysics*, 141, 95-105.
- Salamon, A., Hofstetter, A., Garfunkel, Z. and Ron, H., 1996. Seismicity of the eastern Mediterranean region: Perspective from the Sinai subplate. *Tectonophysics*, 263, 293-305.
- Salamon, A., Hofstetter, A., Garfunkel, Z. and Ron, H., 2003. Seismotectonics of the Sinai subplate - The eastern Mediterranean region. *Geophys. J. Int.*, 155, 149-173.
- Shalem, N., 1945. Earthquakes in Jerusalem along its history. *Jerusalem*, 2 (1-3), 22-54 (in Hebrew).
- Shalem, N., 1949. Whitening of the Dead Sea water. *Teva*, B, 86-90 (in Hebrew).
- Shapira, A., 1997. On the seismicity of the Dead Sea basin. In: *The Dead Sea: The lake and its Setting*, T. M. Niemi, Z. Ben-Avraham and J. R. Gat, (eds.) Oxford Univ. Press, 82-85.
- Sitharam, T. G., GovindaRaju, L. and Sridharan, A., 2004. Dynamic properties and liquefaction potential of soils. *Indian Academy of Science, Current Science*, 87 (10), 1370-1378.
- Sneh, A., Bartov, Y. and Rosensaft, M., 1998. Geological Map of Israel 1:200,000. *Isr. Geol. Surv.*
- Steinitz, G., Begin, Z. B. and Gazit-Yaari, N., 2003. Statistically significant relation between radon flux and weak earthquakes in the Dead Sea rift valley. *Geology*, 31 (6), 505-508.
- Tsuchida, H., 1970. Prediction and countermeasure against liquefaction in sand deposits. Abstract of seminar in Japanese Port and Harbor Institute, 3.1-3.33 (in Japanese).
- van Eck, T. and Hofstetter, A. 1990. Fault geometry and spatial clustering of microearthquakes along the Dead-Sea-Jordan rift fault zone. *Tectonophysics*, 180 (1), 15- 27.
- Wachs, D. and Levitte, D. 1981, Earthquake-induced landslides in the Galilee. *Isr. J. Earth Sci.*, 30, 39-43.
- Wachs, D. and Levitte, D. 1984, Earthquake in Jerusalem and the Mount of Olives landslide. *Israel, Land and Nature*, 9 (3): 118-121.

- Wust, H., 1997. The November 22, 1995, Nuweiba earthquake, Gulf of Elat (Aqaba), Post-seismic analysis of failure features and seismic hazard implications. *Isr. Geol. Surv., Rep. GSI/3/97*, 58 p.
- Wust-Bloch, G. H. and Lazar, M. 2004. Aftershock characterization by portable seismic arrays and tectonic implications of the mb 5.1 Kalia earthquake of 11 February 2004. *Isr. Geol. Soc., Annu. Meet., Abstr.*, p. 121.
- Wust, G. and Wachs, D., 2000. Monitoring aseismic slope activity in northern Israel: A key to comprehensive assessment of seismic triggering of landslides. *Isr. Geol. Surv., Current Res.*, 12, 85-93.
- Yechieli, Y., Magaritz, M., Levy, Y., Weber, U., Kafri, U., Woelfli, W. and Bonani, G. 1993. Late Quaternary geological history of the Dead Sea area, Israel. *Quaternary Res.*, 39, 59-67.
- Zilberman, E., Amit, R., Heimann, A. and Porat, N., 2000. Changes in Holocene Paleoseismic activity in the Hula pull-apart basin, Dead Sea Rift, northern Israel. *Tectonophysics*, 321, 237-252.



Photo 1. Open cracks in the alluvial deposits of N. Og, near Qalya coast. The cracks are oriented parallel to the abandoned and the modern shorelines.



Photo 2. Arcuate cracks along a slump margins, Qalya coast.



Photo 3. Open cracks with vertical offset, probably due to differential compaction, in the N. Darga gully near its outlet to the sea. The cracks are oriented oblique to the shoreline.



Photo 4a. Re-opened cracks along the Qalya coast. Pattern of cracks is oblique to the shoreline. Photo was taken the day after the earthquake.



Photo 4b. Re-opened cracks along the Darga coast. Pattern of cracks in this locality is parallel to the shoreline. Photo was taken the day after the earthquake.



Photo 5a: Seismogenic crack superimposed on mud cracks, Darga coast.



Photo 5b. The pattern of the seismogenic crack below the mud crust is not necessarily identical to the pattern of the mud crack, N. Darga.

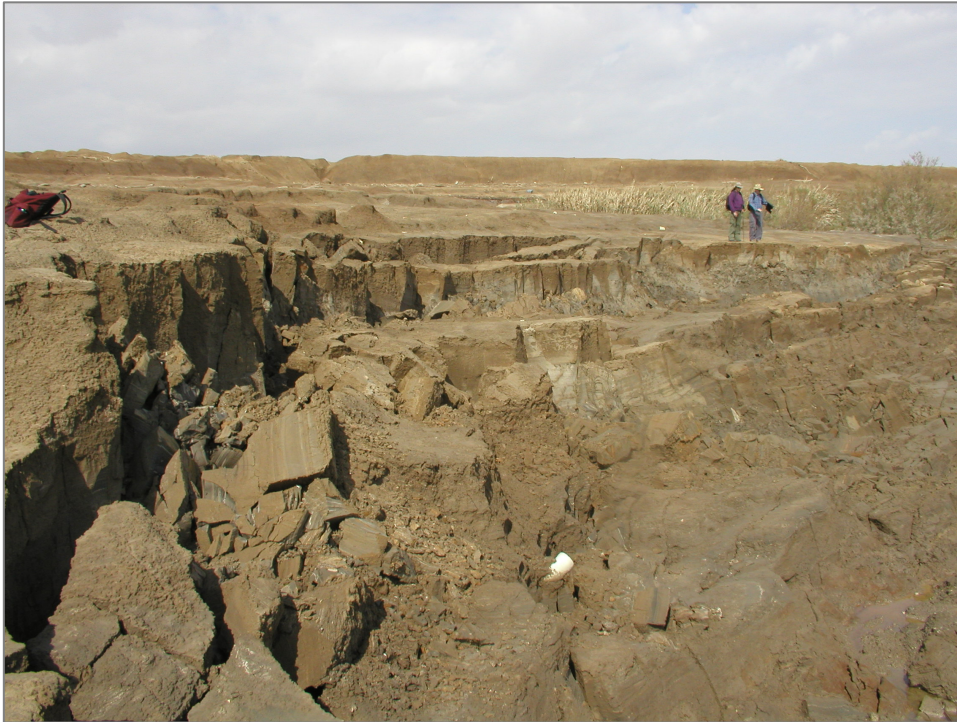


Photo 6a. A slump at the modern sea cliff, Ze'elim Formation, near the waterfront of the Qalya coast. Photo was taken the day after the earthquake.



Photo 6b. Slump of a bank, Ze'elim Formation, in the gully that drains the Hamme En Gedi hot springs. Photo was taken five days after the earthquake (Courtesy of E. Raz).



Photo 7. Collapse of a gully bank of N. Ze'elim, Ze'elim Formation. Photo was taken the day after the earthquake. Note that the collapsed material covers the trace of the flood that occurred a week before the earthquake.



Photo 8. Collapse of the modern sea cliff, Ze'elim Formation, that faces the waterfront of the Qalya coast. Photo was taken the day after the earthquake.

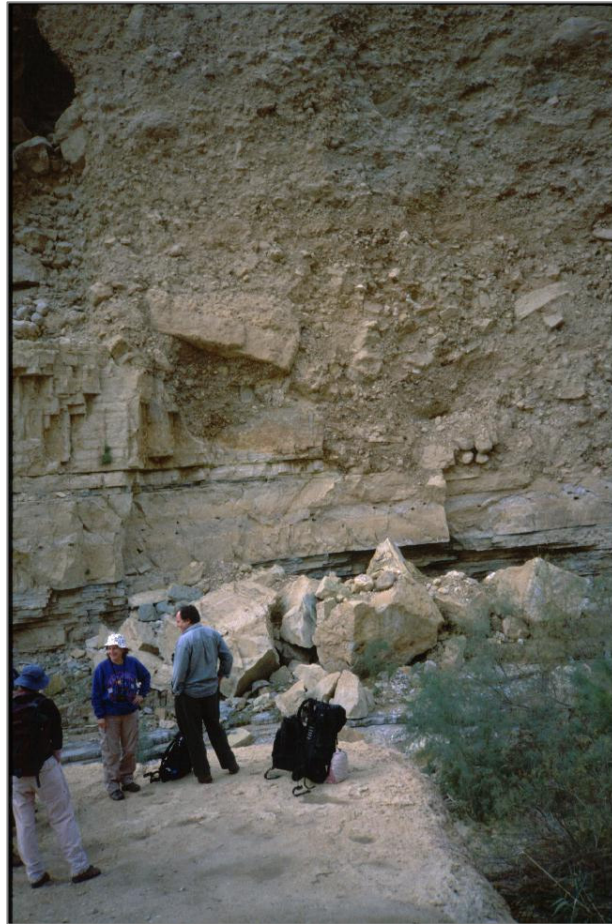


Photo 9. Collapse of fractured hard carbonate rocks of the Judea Group and talus, N. Arugot. Photo was taken in the afternoon, after the earthquake.



Photo 10. The artificial trench near the Qalya coast, where liquefaction and water injection occurred. Note the mud, water and cracks inside the trench. Photo was taken the day after the earthquake.



Photo 11. Mud cones and open cracks inside the artificial trench, near the Qalya coast. The cracks may reflect a very small scale lateral spreading. Photo was taken the day after the earthquake.



Photo 12. Injected mud along an open crack, Darga coast. Photo was taken in the afternoon, after the earthquake.



Photo 13. Wet sediment around a boulder; Darga coast. Photo was taken in the afternoon, after the earthquake.



Photo 14. Waves and an unusual line in the Dead Sea, half an hour after the earthquake. Photo was taken from the Qalya coast looking eastwards (Courtesy of C. Barghoorn, Qalya).



Photo 15. Ponds along the Darga coast, a few meters inland. They seemed to have formed after the earthquake, probably by the run-up wave of the tsunami. Photo was taken in the afternoon, after the earthquake.



Photo 16. Tsunamite deposited by the run-up wave and a re-opened crack, Darga coast. Note the seismite, upper right side of the photo, that was formed by an historical earthquake. Photo was taken a day after the earthquake.



Photo 17a. Ponds in one of the Shalem 2 sinkholes, south of Mineral Beach, Darga coast. Note the small ponds and mud along the margins of the sinkhole. Photo was taken a day after the earthquake.



Photo 17b. Stream lines and open cracks in the mud at the bottom of one of the Shalem 2 sinkholes, south of Mineral Beach, Darga coast. Photo was taken the day after the earthquake.



Photo 18. Turbidity in the Dead Sea, along the coast between En Gedi and the Darga coast. Photo was taken in the afternoon, after the earthquake.

Appendices 1-3

Appendices

Appendix 1 The “INQUA EEE scale”

The new scale is presented here as proposed by Michetti et al. (2004).

Appendix 2 Categories used for the analysis of secondary ground effects

Classification of secondary ground effects used for the evaluation of EEE intensity degree. Secondary effects are defined as such that occur under conditions of precarious equilibrium. These effects need not necessarily be triggered by an earthquake but may also be induced by other natural events or anthropogenic activities. Primary effects, on the other hand, occur under conditions of relatively stable equilibrium and are caused only by an earthquake. See Michetti et al. (2004) for a detailed description.

Appendix 3 INQUA EEE scale field survey form (Michetti et al., 2004)

Appendix 1

The INQUA scale¹

As already mentioned, the assignment of each environmental effect to its proper intensity interval in the following INQUA scale has been based on a careful reading of the most widely applied scales, i.e., the MM, MCS and MSK scales, integrated with more recent work indicated in the references and Appendix 1.

In particular, the diagnostics used in the INQUA scale have been compared and found consistent with the macroseismic data available for a sample of historical and contemporary Italian earthquakes, as listed in Table 2. We have accurately reviewed the surface effects of 115 earthquakes occurred in Italy since the XII century, documented in available catalogs and historical sources directly analyzed. The effects have been categorized according to the scheme in Table 4. Each effect has been associated to the macroseismic intensity attributed in the historical catalogs (Caputo and Faita, 1984; Postpischl, 1985a; 1985b; Boschi *et al.*, 1995; Tinti and Maramai, 1996; Boschi *et al.*, 1997; Azzaro *et al.*, 2001; CPTI, 1999; Boschi *et al.*, 2000) on the basis of local damage patterns.

About the intensity threshold for the occurrence of landslides, we have also taken into account the data of 40 earthquakes worldwide given in Keefer (1984), updated with other 36 events world-wide by Rodriguez *et al.* (1999), and 22 earthquakes in New Zealand (Hancox *et al.*, 2002). For the onset of liquefaction we have also considered the data for Venezuela given in Rodriguez *et al.* (2002).

As for primary faulting, we have based our analysis on a first screening of the Wells and Coppersmith (1994) and Yeats *et al.* (1997) dataset of earthquakes associated to surface faulting, integrated with some recent Italian and Mediterranean region events. The screening has been based on the availability of epicentral intensity values and it is still a work in progress. We have plotted the maximum displacement and the surface rupture length versus epicentral intensity, obtaining the plots in Figure 4.

This database of macroseismic data is subject to expansion and revision in order to incorporate more case histories; however, we are convinced that the sample of seismic events studied is large enough for validating the proposed scale with a resolution consistent with the scope of the present paper. For instance, we found several crustal earthquakes associated with rupture lengths of tens of kilometers for which an epicentral intensity of VIII or even of VII (MM or MSK) has been reported. With the INQUA scale, an epicentral intensity of X or XI would have been assigned, which is unequivocally a better description of the size of these events, both in terms of magnitude and of ground shaking level.

The degrees of the INQUA scale can be directly compared with the corresponding degrees of most of the twelve-degree scales referred to above, in view of the fact that the differences among these scales are not substantial in terms of the level of accuracy they can provide (Appendix 4). The INQUA scale is an innovative proposal — or perhaps is simply the recognition that the work accomplished by earthquake scientists in the first decades of the XX century is worth pursuing along the lines of its original inspiration. It reflects the present viewpoint of its authors, which is necessarily subject to modification in its details, notwithstanding their effort to integrate the largest database possible. Contributions and criticism from other researchers are expected and will be welcomed. They will in all probability provide the basis for a revised version, where new effects may be incorporated and grade intervals of occurrence and size of effects better constrained.

¹ In order to give an immediate identity to this scale, we propose to name it “Inqua EEE Scale”, where EEE would stand for “Earthquake Environmental Effects”.

Definitions of intensity degrees

I, II No perceptible environmental effects

- a) Extremely rare occurrence of small effects detected only from instrumental observations, typically in the far field of strong earthquakes.

III No perceptible environmental effects

- a) Primary effects are absent.
- b) Extremely rare occurrence of small variations in water level in wells and/or the flow-rate of springs, typically in the far field of strong earthquakes.

IV No perceptible environmental effects

- a) Primary effects are absent.
- b) A very few cases of fine cracking at locations where lithology (e.g., loose alluvial deposits, saturated soils) and/or morphology (slopes or ridge crests) are most prone to this phenomenon.
- c) Rare occurrence of small variations in water level in wells and/or the flow-rate of springs.
- d) Extremely rare occurrence of small variations of chemical-physical properties of water and turbidity of water in lakes, springs and wells, especially within large karstic spring systems most prone to this phenomenon.
- e) Exceptionally, rocks may fall and small landslides may be (re)activated, along slopes where equilibrium is already very unstable, e.g. steep slopes and cuts, with loose or saturated soil.
- f) Extremely rare occurrence of karst vault collapses, which may result in the formation of sinkholes, where the water table is shallow within large karstic spring systems.
- g) Very rare temporary sea level changes in the far field of strong earthquakes.
- h) Tree limbs may shake.

V Marginal effects on the environment

- a) Primary effects are absent.
- b) A few cases of fine cracking at locations where lithology (e.g., loose alluvial deposits, saturated soils) and/or morphology (slopes or ridge crests) are most prone to this phenomenon.
- c) Extremely rare occurrence of significant variations in water level in wells and/or the flow-rate of springs.
- d) Rare occurrence of small variations of chemical-physical properties of water and turbidity of water in lakes, springs and wells.
- e) Rare small rockfalls, rare rotational landslides and slump earth flows, along slopes where equilibrium is unstable, e.g. steep slopes, with loose or saturated soil.

- f) Extremely rare cases of liquefaction (sand boil), small in size and in areas most prone to this phenomenon (highly susceptible, recent, alluvial and coastal deposits, shallow water table).
- g) Extremely rare occurrence of karst vault collapses, which may result in the formation of sinkholes, where the water table is shallow within large karstic spring systems.
- h) Occurrence of landslides under sea (lake) level in coastal areas.
- i) Rare temporary sea level changes in the far field of strong earthquakes.
- j) Tree limbs may shake.

VI Modest effects on the environment

- a) Primary effects are absent.
- b) *Occasionally thin, millimetric, fractures are observed in loose alluvial deposits and/or saturated soils; along steep slopes or riverbanks they can be 1-2 cm wide. A few minor cracks develop in paved (asphalt / stone) roads.*
- c) Rare occurrence of significant variations in water level in wells and/or the flow-rate of springs.
- d) Rare occurrence of variations of chemical-physical properties of water and turbidity of water in lakes, springs and wells.
- e) Rockfalls and landslides up to ca. 103 m³ can occur, especially where equilibrium is unstable, e.g. steep slopes and cuts, with loose / saturated soil, or weathered / fractured rocks. The area affected by them is usually less than 1 km².
- f) *Rare cases of liquefaction (sand boil), small in size and in areas most prone to this phenomenon (highly susceptible, recent, alluvial and coastal deposits, shallow water table).*
- g) Extremely rare occurrence of karst vault collapses, which may result in the formation of sinkholes.
- h) Occurrence of landslides under sea level in coastal areas.
- i) Occasionally significant waves are generated in still waters.
- j) *In wooded areas, trees shake; a very few unstable limbs may break and fall, also depending on species and state of health.*

VII Appreciable effects on the environment

- a) Primary effects observed very rarely. Limited surface faulting, with length of tens of meters and centimetric offset, may occur associated with volcano-tectonic earthquakes.
- b) *Fractures up to 5-10 cm wide are observed commonly in loose alluvial deposits and/or saturated soils; rarely in dry sand, sand-clay, and clay soil fractures up to 1 cm wide. Centimetric cracks common in paved (asphalt or stone) roads.*
- c) Rare occurrence of significant variations in water level in wells and/or the flow rate of springs. Very rarely, small springs may temporarily run dry or be activated.
- d) Quite common occurrence of variations of chemical-physical properties of water and turbidity of water in lakes, springs and wells.
- e) Scattered landslides occur in prone areas; where equilibrium is unstable (steep slopes of loose / saturated soils; rock falls on steep gorges, coastal cliffs) their size is sometimes

significant ($10^3 - 10^5 \text{ m}^3$); in dry sand, sand-clay, and clay soil, the volumes are usually up to 100 m^3 . Ruptures, slides and falls may affect riverbanks and artificial embankments and excavations (e.g., road cuts, quarries) in loose sediment or weathered / fractured rock. The affected area is usually less than 10 km^2 .

- f) *Rare cases of liquefaction, with sand boils up to 50 cm in diameter, in areas most prone to this phenomenon (highly susceptible, recent, alluvial and coastal deposits, shallow water table).*
- g) Possible collapse of karst vaults with the formation of sinkholes, even where the water table is deep.
- h) Occurrence of significant landslides under sea level in coastal areas.
- i) Waves may develop in still and running waters.
- j) In wooded areas, trees shake; several unstable branches may break and fall, also depending on species and state of health.

VIII Considerable effects on the environment

- a) *Primary effects observed rarely. Ground ruptures (surface faulting) may develop, up to several hundred meters long, with offsets generally smaller than 5 cm, particularly for very shallow focus earthquakes, such as volcano-tectonic events. Tectonic subsidence or uplift of the ground surface with maximum values on the order of a few centimeters may occur.*
- b) *Fractures up to 25 - 50 cm wide are commonly observed in loose alluvial deposits and/or saturated soils; in rare cases fractures up to 1 cm can be observed in competent dry rocks. Decimetric cracks common in paved (asphalt or stone) roads, as well as small pressure undulations.*
- c) *Springs can change, generally temporarily, their flow-rate and/or elevation of outcrop. Some small springs may even run dry. Variations in water level are observed in wells.*
- d) *Water temperature often change in springs and/or wells. Water in lakes and rivers frequently becomes muddy, as well as in springs.*
- e) Small to moderate ($10^3 - 10^5 \text{ m}^3$) landslides widespread in prone areas; rarely they can occur also on gentle slopes; where equilibrium is unstable (steep slopes of loose / saturated soils; rock falls on steep gorges, coastal cliffs) their size is sometimes large ($10^5 - 10^6 \text{ m}^3$). Landslides can occasionally dam narrow valleys causing temporary or even permanent lakes. Ruptures, slides and falls affect riverbanks and artificial embankments and excavations (e.g., road cuts, quarries) in loose sediment or weathered / fractured rock. The affected area is usually less than 100 km^2 .
- f) *Liquefaction may be frequent in the epicentral area, depending on local conditions; sand boils up to ca. 1 m in diameter; apparent water fountains in still waters; localised lateral spreading and settlements (subsidence up to ca. 30 cm), with fissuring parallel to waterfront areas (river banks, lakes, canals, seashores).*
- g) Karst vaults may collapse, forming sinkholes.
- h) Frequent occurrence of landslides under the sea level in coastal areas.
- i) Significant waves develop in still and running waters.
- j) *Trees shake vigorously; some branches or rarely even tree-trunks in very unstable equilibrium may break and fall.*
- k) *In dry areas, dust clouds may rise from the ground in the epicentral area.*

IX Natural effects leave significant and permanent traces in the environment

- a) *Primary effects observed commonly. Ground ruptures (surface faulting) develop, up to a few km long, with offsets generally smaller than 10 - 20 cm. Tectonic subsidence or uplift of the ground surface with maximum values in the order of a few decimeters may occur.*
- b) *Fractures up to 50 - 100 cm wide are commonly observed in loose alluvial deposits and/or saturated soils; in competent rocks they can reach up to 10 cm. Significant cracks common in paved (asphalt or stone) roads, as well as small pressure undulations.*
- c) *Springs can change their flow-rate and/or elevation of outcrop to a considerable extent. Some small springs may even run dry. Variations in water level are observed in wells.*
- d) *Water temperature often change in springs and/or wells. Water in lakes and rivers frequently become muddy.*
- e) *Landsliding widespread in prone areas, also on gentle slopes; where equilibrium is unstable (steep slopes of loose / saturated soils; rock falls on steep gorges, coastal cliffs) their size is frequently large (10^5 m^3), sometimes very large (10^6 m^3). Landslides can dam narrow valleys causing temporary or even permanent lakes. Riverbanks, artificial embankments and excavations (e.g., road cuts, quarries) frequently collapse. The affected area is usually less than 1000 km^2 .*
- f) *Liquefaction and water upsurge are frequent; sand boils up to 3 m in diameter; apparent water fountains in still waters; frequent lateral spreading and settlements (subsidence of more than ca. 30 cm), with fissuring parallel to waterfront areas (river banks, lakes, canals, seashores).*
- g) *Karst vaults of relevant size collapse, forming sinkholes.*
- h) *Frequent large landslides under the sea level in coastal areas.*
- i) *Large waves develop in still and running waters. Small tsunamis may reach the coastal areas with tidal waves up to 50 - 100 cm high.*
- j) *Trees shake vigorously; branches or even tree-trunks in unstable equilibrium frequently break and fall.*
- k) *In dry areas dust clouds may rise from the ground.*
- l) *In the epicentral area, small stones may jump out of the ground, leaving typical imprints in soft soil.*

X Environmental effects become dominant

- a) *Primary ruptures become leading. Ground ruptures (surface faulting) can extend for several tens of km, with offsets reaching 50 - 100 cm and more (up to ca. 1-2 m in case of reverse faulting and 3-4 m for normal faulting). Gravity grabens and elongated depressions develop; for very shallow focus earthquakes, such as volcano-tectonic events, rupture lengths might be much lower. Tectonic subsidence or uplift of the ground surface with maximum values in the order of few meters may occur.*
- b) *Large landslides and rock-falls ($> 10^5 - 10^6 \text{ m}^3$) are frequent, practically regardless to equilibrium state of the slopes, causing temporary or permanent barrier lakes. River banks, artificial embankments, and sides of excavations typically collapse. Levees and earth dams may even incur serious damage. The affected area is usually up to 5000 km^2 .*
- c) *Many springs significantly change their flow-rate and/or elevation of outcrop. Some may run dry or disappear, generally temporarily. Variations in water level are observed in wells.*

- d) Water temperature often change in springs and/or wells. Water in lakes and rivers frequently become muddy.
- e) *Open ground cracks up to more than 1 m wide are frequent, mainly in loose alluvial deposits and/or saturated soils; in competent rocks opening reach several decimeters. Wide cracks develop in paved (asphalt or stone) roads, as well as pressure undulations.*
- f) *Liquefaction, with water upsurge and soil compaction, may change the aspect of wide zones; sand volcanoes even more than 6 m in diameter; vertical subsidence even > 1m; large and long fissures due to lateral spreading are common.*
- g) Large karst vaults collapse, forming great sinkholes.
- h) Frequent large landslides under the sea level in coastal areas.
- i) *Large waves develop in still and running waters, and crash violently into the shores. Running (rivers, canals) and still (lakes) waters may overflow from their beds. Tsunamis reach the coastal areas, with tidal waves up to a few meters high.*
- j) Trees shake vigorously; branches or even tree-trunks very frequently break and fall, if already in unstable equilibrium.
- k) In dry areas, dust clouds may rise from the ground.
- l) *Stones, even if well anchored in the soil, may jump out of the ground, leaving typical imprints in soft soil.*

XI Environmental effects become essential for intensity assessment

- a) *Primary surface faulting can extend for several tens of km up to more than 100 km, accompanied by offsets reaching several meters. Gravity graben, elongated depressions and pressure ridges develop. Drainage lines can be seriously offset. Tectonic subsidence or uplift of the ground surface with maximum values in the order of numerous meters may occur.*
- b) *Large landslides and rock-falls ($> 10^5 - 10^6 \text{ m}^2$) are frequent, practically regardless to equilibrium state of the slopes, causing many temporary or permanent barrier lakes. River banks, artificial embankments, and sides of excavations typically collapse. Levees and earth dams incur serious damage. Significant landslides can occur at 200 – 300 km distance from the epicenter. Primary and secondary environmental effects can be observed over territory as large as 10000 km².*
- c) Many springs significantly change their flow-rate and/or elevation of outcrop. Frequently, they may run dry or disappear altogether. Variations in water level are observed in wells.
- d) Water temperature often change in springs and/or wells. Water in lakes and rivers frequently becomes muddy.
- e) *Open ground cracks up to several meters wide are very frequent, mainly in loose alluvial deposits and/or saturated soils. In competent rocks they can reach 1 m. Very wide cracks develop in paved (asphalt or stone) roads, as well as large pressure undulations.*
- f) *Liquefaction changes the aspect of extensive zones of lowland, determining vertical subsidence possibly exceeding several meters, numerous large sand volcanoes, and severe lateral spreading features.*
- g) Very large karst vaults collapse, forming sinkholes.
- h) Frequent large landslides under the sea level in coastal areas.
- i) *Large waves develop in still and running water, and crash violently into the shores. Running (rivers, canals) and still (lakes) waters may overflow from their beds. Tsunamis reach the coastal areas with tidal waves up to many meters high.*

- j) *Trees shake vigorously; many tree branches break and several whole trees are uprooted and fall.*
- k) In dry areas dust clouds may arise from the ground.
- l) *Stones and small boulders, even if well anchored in the soil, may jump out of the ground leaving typical imprints in soft soil.*

XII Environmental effects are now the only tool enabling intensity to be assessed

- a) *Primary surface faulting can extend for several hundreds of km up to 1000 km, accompanied by offsets reaching several tens of meters. Gravity graben, elongated depressions and pressure ridges develop. Drainage lines can be seriously offset. Landscape and geomorphological changes induced by primary effects can attain extraordinary extent and size (typical examples are the uplift or subsidence of coastlines by several meters, appearance or disappearance from sight of significant landscape elements, rivers changing course, origination of waterfalls, formation or disappearance of lakes).*
- b) *Large landslides and rock-falls ($> 10^5 - 10^6 \text{ m}^3$) are frequent, practically regardless to equilibrium state of the slopes, causing many temporary or permanent barrier lakes. River banks, artificial embankments, and sides of excavations typically collapse. Levees and earth dams incur serious damage. Significant landslides can occur at more than 200 – 300 km distance from the epicenter. Primary and secondary environmental effects can be observed over territory larger than 50000 km².*
- c) Many springs significantly change their flow-rate and/or elevation of outcrop. Frequently, they may run dry or disappear altogether. Variations in water level are observed in wells.
- d) Water temperature often changes in springs and/or wells. Water in lakes and rivers frequently becomes muddy.
- e) *Ground open cracks are very frequent, up to one meter or more wide in the bedrock, up to more than 10 m wide in loose alluvial deposits and/or saturated soils. These may extend up to several kilometers in length.*
- f) *Liquefaction occurs over large areas and changes the morphology of extensive flat zones, determining vertical subsidence exceeding several meters, widespread large sand volcanoes, and extensive severe lateral spreading features.*
- g) Very large karst vaults collapse, forming sinkholes.
- h) Frequent very large landslides under the sea level in coastal areas.
- i) *Large waves develop in still and running water, and crash violently into the shores. Running (rivers, canals) and still (lakes) waters overflow from their beds; watercourses change the direction of flow. Tsunamis reach the coastal areas with tidal waves up to tens of meters high.*
- j) Trees shake vigorously; many tree branches break and many whole trees are uprooted and fall.
- k) In dry areas dust clouds may arise from the ground.
- l) *Even large boulders may jump out of the ground leaving typical imprints in soft soil.*

Appendix 2

Table 4: Categories used for the analysis of secondary earthquake ground effects

<i>Class of effect</i>	<i>subset</i>
Hydrological anomalies	<ul style="list-style-type: none">• Hydrological discharge rate/water level change• Hydrological-chemical-physical changes and turbidity• New springs• River overflows and lake seiches• Temporary sea level changes - tsunamis
Liquefaction and vertical movements	<ul style="list-style-type: none">• Liquefaction and lateral spreading• Soil and backfilling compaction• Tectonic subsidence/uplift
Landslides (based on Table II in Keefer, 1984)	<ul style="list-style-type: none">• Landslides in rock: rockfalls, rock slides, rock avalanches, rock slumps, rock block slides• Landslides in soil: soil falls, soil slides, soil avalanches, soil slumps, soil block slides, slow earth flows, soil lateral spreads, rapid soil flows, subaqueous landslides• karst vault collapses and sinkholes
Ground cracks	<ul style="list-style-type: none">• Paved roads• Stiff ground• Loose sediments – wet soil

Appendix 3

Notes on the application of the Inqua EEE scale

This document is a first draft proposal of a form aimed at summarizing in the field the main elements characterizing each environmental effect of an earthquake, so that a local intensity can be assigned to the site.

Instructions on how to use this form are not provided here, being most of the keys self-explaining (hopefully). The form is conceived in such a way to be filled in the field with a minimum effort even by a not trained specialist, although a specific experience is highly advisable.

At this stage, all the information has been packed in a single double-faced sheet. However, more information (sketches, notes, photographs) can be provided in additional sheets. Anyway, a longer form may be adopted in the future, if needed. Another goal of the working group is the realization of a sort of database of environmental effects of earthquakes, so changes to this draft form might result necessary to make it more suitable to this end.

Critical evaluation by earthquake geologists, especially by their field testing during surveys after an earthquake, is clearly necessary to bring this draft form to a factual efficiency. To this end it is proposed here. Feedback is therefore not only expected, but it will be greatly welcome.



Earthquake

Region _____ Time _____ Magnitude *MI Ms Mb Mw* _____
Intensity *MM EMS MSK JMA* _____ Latitude _____ Longitude _____ datum _____

Observation point

Nr. _____ Date/hour _____ Surveyor _____ Locality _____

Lat _____ Lon _____ Km from epicentre _____ Local Intensity *MM EMS* _____ Site PGA _____ Photos *yes no*

Geomorphological setting - *mountain slope – mountain valley – hillslope – alluvial fan – bajada – delta - alluvial plain – marsh - sea/river cliff – river/lake bank – sea/lake shore - arid-semiarid flat – desert - other:* _____

Brief description _____

Main effects of seism on artefacts *damage/collapse of single/multiple buildings bridge viaduct tunnel railway highway paved/unimproved road* _____

Environmental effect

Geologic

origin: *tectonic / ground shaking*

newly formed / reactivated

Surface faulting – open fissures in bedrock - mole track - ground crack - slope movement - sinkhole - ground settling/liquefaction/lateral spread - hydrologic anomaly - gas emission - moved/overturnd stone

Other _____

Non geologic *noise light-emission fire vegetation: burnt grass, swinging trees, broken branches, fallen fruits...*

Brief description _____

Major affected lithology rock *densely cleaved massive stratified intrusive metamorphic volcanic lava/pyroclastic sedimentary shale/sandstone/conglomerate/limestone/salt hard/semi-pseudo-coherent – loose sediment soil/clay/silt/sand/gravel colluvium backfill – Sedimentary environment marine shore fan deltaic alluvial lacustrine marsh slope arid/temperate/humid*

Notes _____

Frequency of observed feature in the area

single/multiple number _____ over _____ km² *Already/never* triggered by earthquakes

Maximum dimension length _____m width _____m area _____m² volume _____m³

Average dimension length _____m width _____m area _____m² volume _____m³

Notes _____

Sketch





Earthquake
Environmental
Effects

EEE
Scale

Earthquake Region _____ Time _____
Observation point
 Nr. _____ Date/hour _____ Surveyor _____ Locality _____

Surface faulting strike _____ dip _____
 normal/reverse/oblique/strike-slip dextral/sinistral - total length _____ km - nr of segments ____ - aligned/en-echelon right/left stepping
 maximum vertical offset _____ cm horizontal offset _____ cm - average vertical offset _____ cm horizontal offset _____ cm
 displaced feature for direct measurement _____
 single/multiple scarp – other features *push-up/pull-apart/gravity graben*
 Notes _____

Ground cracks
Type fracture - mole track strike _____ dip _____ Displacement _____ cm sense of displacement _____
 Maximum length _____ m - number of features _____ over a distance of _____ m – maximum opening _____ cm
Shape straight/sinuuous/curvilinear _____ - **Possible origin** surface faulting/slide/ground settling/detachment
 Notes _____

Slope movement
Type rock fall – deep-seated slide (sackung) - rotational slide – slump - earth flow - soil slip – other _____
 Maximum dimension of blocks _____ m³ over a distance of _____ m – Total volume _____ m³ - **Humidity** *very/moderately/no wet*
Age *very old/recent/new* **Activity** *partial/total already active/quiescent*
Velocity *extremely/very/moderately rapid/slow* **Time delay** for manifestation of motion _____ hours
 Notes _____

Ground settlement - collapse
Type liquefaction – compaction – lateral spread - subsidence – bulge – sinkhole – other _____
 Maximum diameter _____ m - number of features _____ over a distance of _____ m – maximum lowering/uplift _____ cm
Shape round/elliptical/elongated/squared _____ positive/negative cone - **Humidity** *very/moderately/no wet*
Depth of water table _____ m – water/sand ejection –
Velocity *extremely/very/moderately rapid/slow* **Time delay/advance** for manifestation of feature _____ hours
 Notes _____

Hydrologic anomaly
Effects *overflow/drying up/appearance of springs/waves/water fountain/variation of water table/discharge rate/temperature/chemistry/turbidity* **where** *spring/river /lake/well/fountain/aqueduct* other _____
 Temperature change _____ C° – Discharge change _____ l/s
 Changed chemical component/s _____ - Permanent/temporary change lasted for _____ hours
Tsunami: maximum wave height _____ m length _____ m Extent of affected coast _____ km
Velocity *extremely/very/moderately rapid/slow* - **Time delay/advance** for manifestation of feature _____ hours
 Notes _____

Intensity attribution IV V VI VII VIII IX X XI XII

Based principally on existing INQUA tables/other Intensity scale/new assessment and _____

תקציר

רעידת אדמה בינונית במגניטודה $M_L=5.2$ התרחשה בצפון מזרח ים המלח, בתאריך 11/2/2004, בשעה 15:10 בבוקר על פי השעון המקומי. מוקד הרעידה היה בעומק 17 ק"מ והמנגנון המכני שחושב עבורה מראה גזירה משולבת במתיחה, בהתאמה כללית עם המשטר הטקטוני בבקע ים המלח. אולם המישורים שהתקבלו בפתרון המכני, האחד בכיוון צפון-צפון-מערב והשני בכיוון מערב, אינם משתלבים בפשטות עם מבנה טקטוני מוכר בתוך אגן ים המלח. רעידות המשנה אירעו ממערב למוקד הרעידה העיקרית, מפוזרות בכיוון מערב-צפון-מערב, ובכך תומכות בהעדפתו של המישור בכיוון מערב כהעתק שפעל. אם כך הדבר, הרי שזה מצביע על מבנה פנימי באגן ים המלח שיצר את הרעידה.

סריקת החוף הצפון מערבי של ים המלח והאזור הדרומי של נהר הירדן העלתה כי הרעידה יצרה מגוון רחב של תופעות גיאולוגיות בעיקר בסלעים הרכים והפריכים של תצורת צאלים ההולוקנית, עד למרחק של כ-40 ק"מ מהמוקד. התופעות העיקריות שנצפו הן:

- א. סדקים: נמצאו ברצועת החוף בין קליה ונחל דרגה, רובם קשורים לתנועות גרביטטיביות לכיוון הים, הידוק של משקעים צעירים ופתיחה מחדש של סדקים קיימים.
 - ב. גלישות, התמוטטויות ומפולות: נצפו לאורך מצוק החוף הטרי בין קליה לעין פשחה ולגדות אחד הערוצים של נחל צאלים בקרבת קו החוף. עוד דווח על נפילות של סלעים בודדים במדרונות תלולים.
 - ג. התנזלות: שלוליות של מים וקונוסים של בוץ נמצאו בחומר מילוי תחוח בתחתית תעלה מלאכותית ליד חוף קליה. בחוף דרגה נצפו בוץ לאורך סדקים שנוצרו ברעידה ורטיבות מסביב לכמה סלעים גדולים.
 - ד. צונאמי: בגובה של עד כמטר וים רוגש נצפו בצפון מזרח ים המלח מיד לאחר הרעידה. יתכן כי שלוליות מים וחלוקים שנמצאו באתרים מסוימים לאורך חוף דרגה מעידים גם הם על נחשול ים.
 - ה. מפלסי מים: במספר בארות לאורך החוף נמדדה למחרת הרעידה עליה של עד כ-30 סמ' במפלס ובבארות אחרות נרשמה ירידה, ביחס למדידות שנעשו כשבועיים לפני האירוע. שפיעת המים בעיינות צוקים גברה. בכמה בולענים באתר שלם 2 ירד מפלס המים במטר. על פי העדויות ירידת המפלס הייתה דרסטית והתרחשה בזמן הרעידה. בהעדר רישום רציף לא ניתן לקבוע מתי אירעו שינויי המפלס ביחס לרעידה.
 - ו. שפיעת רדון: שינוי בשפיעה היומית נרשם בשני חיישנים בעיינות צוקים, כ-10-14 שעות לפני הרעידה.
 - ז. תופעות נוספות: אבק נצפה לאורך החוף הצפון מזרחי של ים המלח בצד הירדני. אנשים דווחו על רעש חזק בעת הרעידה ואחרים ראו תנועה גלית בפני השטח. עצי תמר נעו.
- חלק מהתופעות מתרחשות באזור גם ללא רעידת אדמה, כלומר תנאי אי יציבות קרובים לכשל קיימים לאורך החוף והרעידה רק האיצה חלק מהם. מרבית תופעות הכשל התרחשו בתצורת צאלים ועל כן נראה שהיא החלשה ביותר באזור מבחינה גיאוטקנית ומכאן שגם הרגישה ביותר לסיכונים סיסמיים. על פי הסולם החדש המוצע על ידי INQUA להערכת תופעות טבע שנגרמו כתוצאה מרעידת אדמה, מגיעה העוצמה המרבית של התופעות לדרגה VI. התצפיות והממצאים מצביעים על החשיבות הרבה לאיתור וניטור התופעות מיד לאחר הרעידה מאחר והן דועכות ונעלמות במהירות.



משרד התשתיות הלאומיות

המכון הגיאולוגי

ממצאים גיאולוגיים מרעידת האדמה במגניטודה 5.2 שהתרחשה בצפון-מזרח ים המלח ב - 11/2/2004

עמוס סלמון

בהשתתפות :

מאיר אבלסון¹, יואב אבני¹, רבקה אמית¹, יהודה אנזל², שלמה אשכנזי¹, זאב ב. בגין¹,
גדעון בר¹, זהר גבירצמן¹, איתי גבריאלי¹, רמי הופשטטר³, רמי ויינברגר¹, עזרא זילברמן¹,
חיים חמו¹, יריב חמיאל¹, טונצ'אי טיימז⁴, סדה יולסאל⁴, יוסף יחיאל¹, עודד כץ¹, און
כרובי¹, טומי מגדלן¹, אורי מליק¹, יואב נחמיאס¹, נעמי פורת¹, לאה פלדמן³, כרמי ציון¹,
גיוש שטיינברג¹ וגדעון שטייניץ¹

¹ המכון הגיאולוגי, מלכי ישראל 30, ירושלים 95501, ישראל

² המכון למדעי כדור הארץ, האוניברסיטה העברית, ירושלים 91904, ישראל

³ המכון הגיאופיסי ת.ד. 182, לוד 71100, ישראל

⁴ אגף סיסמולוגיה, האוניברסיטה הטכנית איסטנבול, משלק 80626, איסטנבול, תורכיה